Available online at www.sciencedirect.com

ScienceDirect

Geochimica et Cosmochimica Acta 139 (2014) 248–266

Geochimica et Cosmochimica Acta

www.elsevier.com/locate/gca

Abundances of presolar silicon carbide grains in primitive meteorites determined by NanoSIMS

Jemma Davidson [a,*], Henner Busemann [a,b], Larry R. Nittler [c], Conel M.O'D. Alexander [c], François-Régis Orthous-Daunay [d], Ian A. Franchi [a], Peter Hoppe [e]

[a] Planetary and Space Sciences, Open University, Walton Hall, Milton Keynes MK7 6AA, UK
[b] School of Earth, Atmospheric and Environmental Sciences, The University of Manchester, Oxford Road, Manchester M13 9PL, UK
[c] Department of Terrestrial Magnetism, Carnegie Institution of Washington, 5241 Broad Branch Road, Washington, DC 20015-1305, USA
[d] Institut de Planétologie et d'Astrophysique de Grenoble, UJF CNRS/INSU, 38000 Grenoble, France
[e] Max-Planck-Institut für Chemie, P.O. Box 3060, 55020 Mainz, Germany

Received 2 February 2014; accepted in revised form 18 April 2014; Available online 9 May 2014

Abstract

It has been suggested that the matrices of all chondrites are dominated by a common material with Ivuna-like (CI) abundances of volatiles, presolar grains and insoluble organic matter (IOM) (e.g., Alexander, 2005). However, matrix-normalized abundances of presolar silicon carbide (SiC) grains estimated from their noble gas components show significant variations in even the most primitive chondrites (Huss and Lewis, 1995; Huss et al., 2003), in contradiction to there being a common chondrite matrix material. Here we report presolar SiC abundances determined by NanoSIMS raster ion imaging of IOM extracted from primitive members of different meteorite groups. We show that presolar SiC abundance determinations are comparable between NanoSIMS instruments located at three different institutes, between residues prepared by different demineralization techniques, and between microtomed and non-microtomed samples. Our derived SiC abundances in CR chondrites are comparable to those found in the CI chondrites (~30 ppm) and are much higher than previously determined by noble gas analyses. The revised higher CR SiC abundances are consistent with the CRs being amongst the most primitive chondrites in terms of the isotopic compositions and disordered nature of their organic matter. Similar abundances between CR1, CR2, and CR3 chondrites indicate aqueous alteration on the CR chondrite parent body has not progressively destroyed SiC grains in them. A low SiC abundance for the reduced CV3 RBT 04133 can be explained by parent body thermal metamorphism at an estimated temperature of ~440 °C. Minor differences between primitive members of other meteorite classes, which did not experience such high temperatures, may be explained by prolonged oxidation at lower temperatures under which SiC grains formed outer layers of SiO_2 that were not thermodynamically stable, leading to progressive degassing/destruction of SiC.

1. INTRODUCTION

Before the discovery of isotopic anomalies in meteorites, the Solar System was widely considered to be an isotopically homogeneous reservoir (Cameron, 1962). However, this proved to be erroneous with the detection of isotopic anomalies (e.g., Signer and Suess, 1963; Reynolds and Turner, 1964), later attributed to the presence of presolar grains (microscopic dust grains formed in the outflows and cooling gases of stars prior to solar system formation) in meteorites (e.g., Lewis et al., 1987; Tang and Anders, 1988). While presolar grains produce isotopic anomalies on the micrometer scale, the material that accreted to form the meteorite parent bodies was physically and chemically

* Corresponding author. Present address: Department of Terrestrial Magnetism, Carnegie Institution of Washington, 5241 Broad Branch Road, Washington, DC 20015-1305, USA. Tel.: +1 202 478 8459.
E-mail address: jdavidson@carnegiescience.edu (J. Davidson).

http://dx.doi.org/10.1016/j.gca.2014.04.026
0016-7037/

heterogeneous on macroscopic scales. These heterogeneities include: short-lived radionuclide abundances, noble gas abundances, oxygen and other stable isotope anomalies, bulk element compositions, size-distributions and relative abundances of components (e.g., chondrules, calcium-, aluminum-rich inclusions (CAIs), matrix, metal grains, and presolar grains). These pre-accretionary heterogeneities could potentially result from processes such as molecular cloud heterogeneity, formation and destruction of dust grains in the solar nebula, fractionation in the nebula involving incomplete evaporation/condensation or size/density sorting, etc. However, there is evidence that matrix material was a relatively well-mixed reservoir throughout the chondrite forming region, at least in terms of the abundances of volatile elements, presolar grains and organic matter (e.g., Huss and Lewis, 1995; Alexander et al., 2001, 2007; Alexander, 2005; Busemann et al., 2007; Zanda et al., 2009, 2012). Since presolar grains and IOM-like (insoluble organic matter; a major component of organic matter in chondrites) material, along with amorphous silicates, enstatite whiskers and plates, and fine-grained compositionally heterogeneous olivine (Ishii et al., 2008; Zolensky et al., 2008), are present in chondrite matrices, interplanetary dust particles and comets, it seems likely that this matrix material was widely distributed in the solar nebula.

As presolar grains predate any solar nebula processes, one way to probe the heterogeneity at the formation of the inner Solar System/asteroid belt is to survey their abundances in primitive members of the various chondrite groups. Such a survey would address: (i) the distribution of presolar grains throughout the meteorite-forming regions of the early Solar System, and (ii) the effects of aqueous and thermal alteration within meteorite classes.

Presolar grains (including silicates, oxides, nanodiamonds, graphite, and silicon carbide) were incorporated into all chondrite classes and can be found in the most primitive members (i.e., least thermally altered) of each (e.g., Huss and Lewis, 1995; Huss et al., 2003; Zinner, 2014). Primitive chondrites also contain abundant carbonaceous material (2–4 wt.%), most of which is present as IOM (e.g., Gilmour, 2003). Of all chondrite classes, CI chondrites most closely match the elemental composition of the solar photosphere and thus are closest in composition to the starting material of the early Solar System. After parent body formation, all chondrites were subjected to thermal and/or hydrothermal processes (Brearley, 2006; Huss et al., 2006), the effects of which are evident in the systematic changes in abundances and properties of what remains of the original IOM and presolar grains (Huss et al., 2003, 2006; Quirico et al., 2003, 2005; Alexander, 2005; Bonal et al., 2006; Alexander et al., 2007; Busemann et al., 2007). Also, presolar grains and IOM would not have survived chondrule or CAI formation, so not surprisingly they are found exclusively in the matrix (e.g., Floss and Stadermann, 2005, 2009a,b; Nguyen et al., 2007, 2010; Davidson, 2009; Bose et al., 2012; Leitner et al., 2012a) and fine-grained chondrule rims (e.g., Davidson, 2009; Davidson et al., 2012a; Haenecour and Floss, 2012; Leitner et al., 2012a,b). After taking into account variations in parent body modification, Alexander (2005) argued that the relative abundances of presolar grains and IOM, and their matrix-normalized absolute abundances are roughly CI-like in all chondrites. However, presolar grain abundance estimates based on noble gas contents are inconsistent with this (Huss and Lewis, 1995; Huss et al., 2003).

Presolar nanodiamond, silicon carbide (SiC) and graphite were all identified because they contain relatively high abundances of isotopically anomalous noble gases (e.g., Anders and Zinner, 1993). Noble gases can be used as tracers of presolar grain abundances in bulk meteorites (e.g., Huss, 1990; Huss and Lewis, 1995; Huss et al., 2003) provided that the presolar grains in different meteorites contain uniform amounts of the anomalous noble gas components and that the concentrations of these components are well determined for each grain type. Nanodiamonds, carriers of the isotopically anomalous Xe-HL, are the smallest (~2.5 nm diameter) and most abundant type of presolar grain (~1400 ppm; Zinner, 2014). Their small size requires that isotopic compositions be determined by measurements of large grain aggregates. Xenon-HL is thought to have been produced in supernovae and is rare in nanodiamonds (only ~one in a million diamond grains contains a single Xe atom; Huss and Lewis, 1994). Consequently, only a tiny fraction of the nanodiamonds is demonstrably presolar in origin (Nittler, 2003 and references therein).

The abundances of presolar SiC grains estimated from their noble gas components show considerable variations in even the most primitive chondrites (<2 to 29 ppm; Huss and Lewis, 1995; Huss et al., 2003). This contradicts the idea that a well-mixed reservoir of presolar grains was incorporated into the matrices of all primitive chondrite classes. In particular, Huss et al. (2003) determined that the primitive CR (Renazzo-like) carbonaceous chondrites (only Renazzo was analyzed) have matrix-normalized SiC abundances that are much lower (<2 ppm) than those of the CI group (~29 ppm). Because of apparent correlations between SiC abundances and moderately volatile element fractionations in their host chondrites, Huss et al. (2003) suggested that the low SiC abundances in CRs were due to high temperatures (possibly > 700 °C) experienced by the precursor material of the CR matrices in the solar nebula.

High bulk H/C ratios, δD and $\delta^{15}N$ values, and C Raman characteristics show that the CR chondrites contain the most primitive IOM of any chondrite class (Busemann et al., 2006, 2007; Alexander et al., 2007). Nuclear magnetic resonance (NMR) spectroscopy and elemental analysis also show that the CR IOM is the most aliphatic IOM found in any chondrites (Cody and Alexander, 2005; Alexander et al., 2007), implying that they experienced very little heating. Based on the presence of large H and N isotopic anomalies, the IOM is believed to have formed in the interstellar medium or in the cold outer regions of the solar nebula (Robert and Epstein, 1982; Yang and Epstein, 1983, 1984; Kerridge, 1983; Busemann et al., 2006; Pizzarello et al., 2006; Alexander et al., 2007). The IOM would have been strongly modified or destroyed by sustained temperatures of ⩾400 °C. MicroRaman and X-ray absorption spectroscopy studies suggest, however that the IOM in CR

chondrites experienced peak temperatures of less than 240 °C (Busemann et al., 2007; Cody et al., 2008).

Thus, either the CR chondrite IOM somehow escaped the nebular heating event(s) proposed by Huss and Lewis (1995), implying that it was mixed with SiC post-heating, or SiC was somehow degassed/destroyed at low temperatures. Huss (1990), Huss and Lewis (1995) and Huss et al. (2003) showed that noble gas abundances in chondrites decrease with increasing metamorphism, presumably because metamorphism progressively degassed or destroyed their presolar grain hosts. This metamorphic degassing/destruction can be seen in meteorites whose estimated peak metamorphic temperatures are much less than 700 °C. In the meteorite parent bodies, the presence of oxidants and a fluid to enhance diffusion and reaction may make it possible to degas/destroy the SiC grains at relatively low temperatures (Alexander et al., 1990a; Russell et al., 1997).

Since the apparent conflict, particularly in CRs, between SiC abundances as determined from noble gases and IOM primitiveness could simply be due to low temperature degassing of the SiC, it is necessary to determine presolar SiC abundances directly and independently of noble gases. This study aims to achieve this with the use of direct raster ion imaging by secondary ion mass spectrometry (SIMS) utilizing the high spatial resolution of the NanoSIMS ion microprobe. Both X-ray mapping in the scanning electron microscope and SIMS-based ion imaging have been used successfully to locate presolar SiC grains *in situ* in meteorites and interplanetary dust particles (IDPs) (e.g., Alexander et al. 1990b; Stadermann et al., 2006; Busemann et al., 2009; Davidson et al., 2012b). However, presolar SiC abundances even in matrix are low (10s ppm or less) and SiC in thin sections is susceptible to contamination and plucking. In this study, we have chosen to work with IOM-rich residues rather than thin sections. SiC abundances in these residues are $\geqslant$50 times enriched compared to bulk meteorites, thereby greatly reducing the total areas that must be mapped to locate statistically significant numbers of grains and thus allowing us to analyze primitive meteorites from several other chondrite groups in addition to the pivotal CR chondrites.

2. ANALYTICAL PROCEDURE

2.1. Sample selection

IOM separates were selected from a variety of primitive chondrites. Seven CR chondrite samples were studied here by NanoSIMS ion imaging, including Renazzo (the only CR studied by noble gas analysis to date; Huss et al., 2003). They cover the whole range of aqueous alteration, from the most severely aqueously altered CR1 known (Grosvenor Mountains [GRO] 95577; Weisberg and Huber, 2007), through the CR2s (Al Rais, Renazzo, Graves Nunataks [GRA] 95229, Elephant Moraine [EET] 92042; Weisberg et al., 1993; Abreu, 2007), to the two least altered CR3s (Queen Alexandra Range [QUE] 99177 and Meteorite Hills [MET] 00426; Abreu and Brearley, 2010). Renazzo, GRA 95229, QUE 99177 and MET 00426 have previously been analyzed via NanoSIMS ion imaging of *in situ* matrix (Floss and Stadermann, 2005, 2009a; Nguyen et al., 2010; Leitner et al., 2012a).

The CM2 Murchison was chosen to compare the NanoSIMS method with results obtained by measuring noble gases (Huss et al., 2003), and to compare residues prepared by two different techniques (see below) to determine the effect of sample preparation technique on inferred presolar SiC abundance. Bells (an anomalous CM2) was chosen because of the particularly anomalous H and N isotopic ratios in its IOM (Alexander et al., 2007).

A variety of other particularly primitive chondrites were also selected in order to sample as broad a region of the inner early Solar System as possible, including: Acfer 094 (ungrouped C3; Nagashima et al., 2004), Semarkona (LL3.0; Hutchison et al., 1987; Alexander, 1989) and Allan Hills (ALHA) 77307 (CO3.0; Brearley, 1993). Semarkona and ALHA 77307 were previously analyzed for their noble gases (Huss and Lewis, 1995; Huss et al., 2003), allowing further direct comparison with our new data. ALHA 77307 has also been previously analyzed via NanoSIMS ion imaging of *in situ* matrix (e.g., Nguyen et al., 2007, 2010; Bose et al., 2012). Roberts Massif (RBT) 04133, an Antarctic find originally classified as a CR, is mildly thermally metamorphosed (~3.4 petrologic type) and represents the reduced CV chondrites (Davidson et al., 2009a,b).

2.2. Sample preparation

Most residues, including Murchison "A", were prepared by CsF-HF (1.6–1.7 g/cm^3 and pH ~7) demineralization (Cody et al., 2002; Cody and Alexander, 2005; Alexander et al., 2007). Digestion of silicate minerals occurs entirely at room temperature by utilizing a fluoride salt (here CsF) to provide the principal demineralizing agent (the F^- ion) instead of HF (conventional technique). However, some HF is added to adjust the pH of the solution. A Renazzo IOM residue could not be prepared by the CsF-HF method due to the lack of an available sample. However, we obtained a small amount of residue prepared with the second residue preparation technique (Renazzo; Murchison "B"), which is a variation on the traditional HF-HCl method (Orthous-Daunay et al., 2008, 2010). It is less time intensive (each sample takes ~15–36 h to prepare) and was developed for use with very small samples (~10 μg starting material; Orthous-Daunay et al., 2010; Orthous-Daunay, 2011). The total processing time for Renazzo was 15 h, compared to 36 h for Murchison where a boric acid sequence was added to remove secondary fluorides.

Bells IOM samples were prepared for SIMS imaging by ultramicrotomy with a Leica Ultracut microtome at the Carnegie Institution of Washington (CIW); a diamond knife was used to create ~500 nm thick sections of material that were placed on a gold mount for NanoSIMS analysis (see Cody et al., 2006, for method). For the remaining samples, individual ~10 μm fragments of IOM were picked from glass slides with tungsten micro-needles attached to a Narishige micromanipulator system MMN-1/MMO-202 coupled to a Nikon Eclipse LV-100D microscope, with similar systems installed both at the Open University (OU) and at CIW. For improved conductivity and imaging, the grains

were then placed on, and later pressed into, high-purity gold foils mounted on aluminum stubs. The gold foils were annealed at ~1000 °C prior to sample mount preparation and feature imprints of standard copper TEM grids for orientation.

2.3. NanoSIMS isotopic analysis

Raster ion images of approximately 10–15 grains of IOM (e.g., Fig. 1) were collected per meteorite; most ion images were obtained with the Cameca NanoSIMS 50L instrument at the OU (176 images). Additional images obtained with the CIW (12 images; NanoSIMS 50L) and the Max-Planck-Institut für Chemie, Mainz (MPI; 15 images; NanoSIMS 50) instruments were analyzed for comparative purposes (see Busemann et al., 2006 for experimental details). For most data collected, the IOM fragments were pre-sputtered with probe currents of typically ~100 pA for up to 10 min (depending on fragment size; 20 × 20 μm to 30 × 30 μm raster sizes) until sputter equilibrium was reached. Analyses were undertaken with probe currents of ~1 pA, and raster sizes of usually 15 × 15 μm to 25 × 25 μm (512 × 512 pixels), providing a typical spatial resolution of better than 150 nm. Each fragment was mapped for the following secondary ions simultaneously: $^{12}C^-$, $^{13}C^-$, $^{16}O^-$, $^{12}C^{14}N^-$, $^{12}C^{15}N^-$, $^{28}Si^-$ and one other ion ($^{56}Fe^-$, $^{24}Mg^{16}O^-$ or $^{32}S^-$), as well as secondary electrons, to detect and distinguish presolar SiC from any other anomalous carbonaceous grains that might have been present in the IOM. The mass spectrometer was tuned to provide a mass resolving power ($m/\Delta m$) of >8000 (Cameca definition, see also Hoppe et al., 2013), sufficient to resolve the principle interference peaks for the elements studied (C, N, O), such as hydrides and BO (see also Zinner et al., 1989; Hoppe et al., 1994). Each image consists typically of six planes (repeated scans on the same area) that took a total of ~70 min to collect.

2.4. Data reduction

The data were generated as ion images (or "maps") for each of the isotopes measured, which were then used to create isotope/element ratio maps (Fig. 1b, c). Ion images were processed and quantitatively analyzed with the L'IMAGE software (L.R. Nittler, CIW). Prior to data extraction, individual image planes were aligned with each other to correct for stage and/or beam drift during the measurement. The total areas of the various residues that were imaged were determined from combined ^{12}C, ^{16}O, and secondary electron images. SiC grains were identified by systematically applying suitable minimum threshold values to $^{13}C/^{12}C$ "sigma" images to identify anomalous areas. "Sigma" images display at each pixel the number of standard deviations (based on counting statistics) that the pixel ratio is from the bulk IOM value. Candidate presolar SiC grains were identified based on their exhibiting a $>3\sigma$ anomaly in $^{13}C/^{12}C$, spatially correlated with a $^{28}Si^-/^{12}C^-$ ion ratio that was at least three times greater than that of the bulk IOM fragment (Fig. 1c).

Presolar grain abundances from ion images were calculated by comparing the ratio of the area of the grains to the total area of residue analyzed. Taking into account the mass fraction **Y** of the bulk meteorite in the residues (Alexander et al., 2007) and the density difference between SiC grains and IOM residue, matrix-normalized abundances were calculated from the formula:

$$\mathrm{SiC(ppm)} = \overline{\mathbf{Y}} * \boldsymbol{v} * (\boldsymbol{\rho 1}/\boldsymbol{\rho 2}) * \mathbf{10^6} \quad (1)$$

where $\overline{\mathbf{Y}}$ is the matrix-normalized mass fraction of the IOM residue in the bulk meteorite, $\boldsymbol{v}$ is the area fraction of SiC grains, $\boldsymbol{\rho 1}$ is the density of SiC (3.21 g cm^{-1}), and $\boldsymbol{\rho 2}$ is the density of residue (1.5 g cm^{-1}). Uncertainties in derived SiC abundances are described below in Section 3.4.

2.5. UV-ozone chamber

A UV-ozone chamber at the OU (Sestak et al., 2006) was used to remove IOM material from one meteorite residue (CR3 MET 00426) after NanoSIMS analysis. The experiment was designed to determine what effect mixing with the surrounding IOM has on the size estimates and C isotopic ratios of the presolar SiC grains determined from the NanoSIMS image analysis. This was achieved by re-analyzing the same sample by NanoSIMS ion imaging after

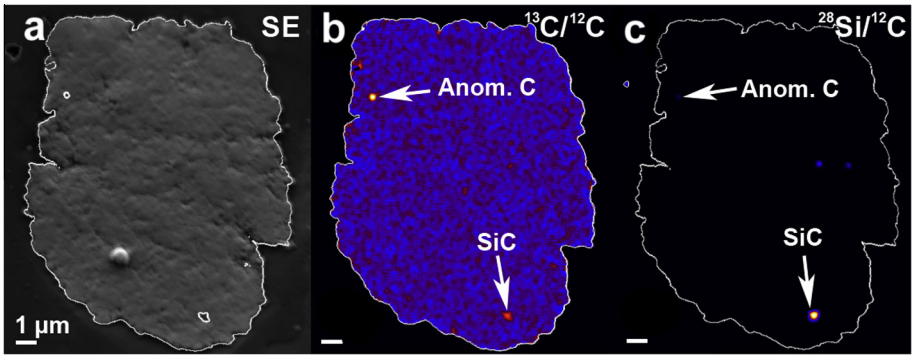

Fig. 1. NanoSIMS ion images of Orgueil (CI) IOM residue fragment #05: (a) secondary electron image, (b) $^{13}C/^{12}C$ map used to identify ^{13}C anomalies that are potential SiC grains, (c) $^{28}Si/^{12}C$ map used to verify presence of SiC grains (in this example only the bottom right grain is SiC) with residue outline. All scale bars are 1 μm.

the removal of IOM by oxidation. The UV-ozone experiment lasted for a total of 6 weeks, during which the UV-lamp and oxygen flow ran for a total of 30 days. High-purity oxygen was gently flowed at ~50 cm^3/min through an elongated stainless steel chamber containing the sample and a low-pressure mercury lamp with strong ultraviolet emission. Emission at 185 nm generates ozone, while emission at 254 nm breaks down the ozone to form highly reactive atomic oxygen and photoactivates the organic material (Sestak et al., 2006).

3. RESULTS

A total of 218 presolar SiC grains were located in 203 NanoSIMS images (excluding post-oxidation data; 177 presolar SiC grains in 196 images) from 14 different meteorites. Before presenting the results in detail, we discuss several aspects of the analysis, including comparisons of results from different laboratories and sample preparation techniques, the results of the UV-ozone experiment and how we estimate uncertainties in the SiC abundances.

3.1. Comparison between NanoSIMS instruments

Data collected for the CR1 carbonaceous chondrite GRO 95577 using all three NanoSIMS instruments employed in this study show that there is no bias between laboratories as the derived presolar SiC abundances agree within error (Table 1). However, one very large (1.26 μm diameter compared to typical diameters of ~300–400 nm) SiC grain skewed the concentration determined with the MPI instrument towards a high SiC abundance (reflected by large errors based on grain counting statistics). Data were also collected at the OU and MPI for the CR2 EET 92042; these abundance estimates agree within error (Table 1).

3.2. Comparison of sample preparation techniques

Data collected from the two different Murchison residues (A and B; Section 2.2) demonstrate that all residues are comparable regardless of their preparation method: neither residue preparation method preferentially destroys SiC grains (Table 1). As a result, data from the CR2 Renazzo residue, prepared with the modified HF-HCl method (Orthous-Daunay et al., 2010), can be compared to data obtained on the other CR chondrite residues that were prepared by the CsF-HF method.

Microtomed and non-microtomed fragments of Bells (anom. CM2) were analyzed to determine the effect of microtoming on presolar SiC abundances (i.e., whether this technique preferentially plucks away hard SiC grains from the surrounding softer IOM). The data show that both the microtomed and non-microtomed samples (measured at the MPI on $\geqslant$1900 μm^2 areas) give almost identical abundances of 30^{+20}_{-13} ppm and 38^{+37}_{-21} ppm, respectively (see Table 1). This result indicates that microtoming does not preferentially "pluck" out robust SiC grains from the softer surrounding IOM.

Since there is agreement between the data from the three NanoSIMS instruments, all data for the same meteorites are combined in order to improve the statistical significance of the calculated abundances (i.e., GRO 95577, EET 92042, Bells; Table 2).

3.3. UV-ozone oxidation experiment

The CR3 chondrite MET 00426 was chosen for the removal of IOM via the UV-ozone oxidation experiment because it is very primitive. During ozone treatment the IOM was mostly removed, leaving exposed presolar SiC grains (Fig. 2). Five areas of MET 00426 IOM were reanalyzed after oxidation, along with an additional two areas that were previously unanalyzed. NanoSIMS analyses prior

Table 1
Matrix-normalized presolar SiC abundances (ppm) for four primitive chondrites analyzed by NanoSIMS ion imaging at the OU = Open University, MPI = Max-Planck-Institut für Chemie, Mainz, and CIW = Carnegie Institution of Washington. The two Murchison (CM2) residues were prepared by different methods (Section 2.2). Bells data are for microtomed and non-microtomed samples.

Meteorite	Sample	Lab.	Area (μm^2)	# Images collected	# SiC grains located	Abundance ppm (mx-norm.)
GRO 95577 (CR1)		OU	4740	17	30	24^{+5}_{-5}
		MPI	1960	2	1	21^{+48}_{-17}
		CIW	1510	6	3	16^{+16}_{-9}
	Total		8210	25	34	22^{+4}_{-4}
EET 92042 (CR2)		OU	5960	22	29	30^{+7}_{-6}
		MPI	660	2	1	18^{+41}_{-15}
	Total		6620	24	30	29^{+6}_{-5}
Murchison (CM2)	A CsF	OU	3280	13	8	13^{+6}_{-4}
	B micro HF/HCl	OU	2280	10	8	10^{+5}_{-3}
	Total		5560	23	16	12^{+4}_{-3}
Bells (anom. CM2)*	Microtomed	MPI	4220	6	5	30^{+20}_{-13}
	Non-microtomed	MPI	1900	4	3	38^{+37}_{-21}
	Total		6120	10	8	33^{+16}_{-11}

* Bells SiC abundances are calculated using a matrix abundance of 63.6 vol.% reported for Murchison which may be more representative than the 81.7 vol.% reported for the heavily brecciated Bells (Alexander et al., 2007; and references therein). Errors are 1σ after Gehrels (1986).

Table 2
Primitive chondrites analyzed here by NanoSIMS ion imaging, their classification, the area of sample analyzed, number of NanoSIMS images taken, number of presolar SiC grains located and resultant matrix-normalized presolar SiC abundances (ppm), estimated error components and final, corrected abundances, and the minimum, maximum, mean (and 1σ standard deviation) diameters (nm) of the presolar SiC grains located. Also shown are matrix-normalized presolar SiC abundances (ppm) determined by noble gas analyses (Huss and Lewis, 1995; Huss et al., 2003). All errors are 1σ (uncertainties for data from Huss and Lewis (1995) have been recalculated to include a 10% calibration error to enable comparison with Huss et al. (2003) data). CR and CM chondrites are listed in approximate order of decreasing aqueous alteration (see Alexander et al., 2007).

(1)	(2) Class	(3) Lab. [a]	(4) Matrix (vol.%)	(5) Area (μm^2)	(6) # Images collected	(7) # SiC grains located	(8) Matrix-normalised abundance (ppm) raw [b]	(9) Abundance corrections: Below beam size (+)	(10) Abundance corrections: Isotopic dilution (+)	(11) Matrix error (+/−)	(12) Combined correction/ error	(13) Mx-norm. abundance (ppm): Corrected SiC abun. (ppm) NanoSIMS [c]	(14) Mx-norm. abundance (ppm): Noble gases [d]	(15) SiC grain sizes: Min. (nm)	(16) SiC grain sizes: Max. (nm)	(17) Mean (nm)	(18) Standard dev.
Carbonaceous chondrites																	
CI																	
Orgueil	CI1	OU	100[f]	3040	13	13	30^{+11}_{-8}	2.2	1.5	0.0	4	34^{+11}_{-8}	14.2 ± 1.9–28.5 ± 5.6	250	530	370	75
CR			*44 ± 17*	*29940*[j]	*103*[j]	*114*[j]	*29 ± 8*	*1.5*	*1.5*	*3.2*	*3 ± 3*	*32 ± 9*		*130*	*830*	*410*	*115*
GRO 95577	CR1	OU/MPI/CIW	65.8[g]	8210	25	34	22^{+4}_{-4}	1.1	1.1	2.5	2 ± 3	24^{+5}_{-5}		270	610	390	90
Al Rais	CR2	OU	68.8[g]	4420	7	12	23^{+9}_{-7}	1.5	1.1	2.6	3 ± 3	26^{+9}_{-7}		300	530	390	70
Renazzo	CR2	OU	36[g]	1920	12	9	31^{+14}_{-10}	2.5	1.6	3.5	4 ± 4	35^{+14}_{-11}	1.86 ± 0.55	220	440	340	100
GRA 95229	CR2	OU	30[g]	4120	19	12	44^{+17}_{-13}	1.7	2.2	4.9	3 ± 5	47^{+18}_{-14}		380	740	500	100
EET 92042	CR2	OU/MPI	28.9[f]	6620	24	30	29^{+6}_{-5}	1.8	1.5	3.3	3 ± 3	32^{+7}_{-6}		130	570	360	100
QUE 99177	CR3	CIW	36.7[g]	1160	6	6	41^{+24}_{-16}	1.2	2.0	4.5	3 ± 5	44^{+24}_{-17}		430	830	550	130
MET 00426	CR3	OU	38.8[g]	3490	10	11	26^{+8}_{-8}	0.9	1.3	2.9	2 ± 3	28^{+9}_{-9}		480	680	580	110
MET 00426 PO[e]	CR3	OU	38.8[g]	2760	7	41								230	550	370	90
CM				*11680*	*33*	*24*	*19 ± 5*	*0.7*	*1.0*	*2.1*	*2 ± 2*	*21 ± 5*					
Murchison	CM2	OU	63.6[f]	5560	23	16	12^{+4}_{-3}	1.0	0.6	1.3	2 ± 1	14^{+4}_{-3}	21.2 ± 2.2	205	620	330	110
Bells	Anom. CM2	MPI	63.6[h]	6120	10	8	33^{+16}_{-11}	0.5	1.6	3.6	2 ± 4	35^{+16}_{-12}		540	1020	770	155
CO																	
ALHA 77307	CO3.0	OU	33.7[f]	7680	12	11	10^{+4}_{-3}	0.5	0.5	1.1	1 ± 1	11^{+4}_{-3}	8.8 ± 1.6	320	600	430	80
CV																	
RBT 04133	CV3	OU	47.2[i]	2390	12	3	4^{+4}_{-2}	0.4	0.2	0.4	1 ± 1	5^{+4}_{-2}		260	380	300	65
Ungrouped																	
Acfer 094	C3	OU	42[f]	2120	7	5	25^{+17}_{-11}	1.0	1.3	2.8	2 ± 3	27^{+17}_{-11}		420	710	490	120
Ordinary chondrite																	
LL																	
Semarkona	LL3.0	OU	15.6[f]	3230	16	7	27^{+15}_{-10}	1.5	1.3	3.0	3 ± 3	30^{+15}_{-10}	10.0 ± 1.6–20.1 ± 4.2	360	480	420	70

The bold and italics indicate averages of various parameters for the CR and CM chondrite groups.

[a] OU = Open University, MPI = Max-Planck-Institut für Chemie, Mainz, CIW = Carnegie Institution of Washington.

[b] Includes 1σ errors based on counting statistics after Gehrels (1986). Overall abundances for different meteorite group are averages of individual meteorite abundances (errors are standard deviations).

[c] Corrected abundance includes initial determined abundance plus estimates for non-detection of grains below the beam size and those that are isotopically normal. Corrected error includes errors based on counting statistics combined with those determined for matrix variability (errors combined in quadrature). Overall abundances for different meteorite group are averages of individual meteorite abundances (errors are standard deviations).

[d] Noble gas data from Huss and Lewis (1995), and Huss et al. (2003). For Orgueil and Semarkona two abundances are reported – the lowest calculated using constant Ne-E(H) and the highest using variable Ne-E(H). Matrix abundances used for normalization are the same as those used for ion imaging data presented here with the exception of Renazzo where 31.1 vol.% was used.

[e] For the CR chondrite MET 00426 "PO" = post-oxidation.

[f] Alexander et al. (2007) and references therein.

[g] Matrix abundances calculated using combined data from Weisberg et al. (1993) and Schrader et al. (2011).

[h] Assumed matrix abundance is the same as Murchison because Bells is heavily brecciated.

[i] Davidson et al. (2009b).

[j] Total values do not include MET 00426 PO data.

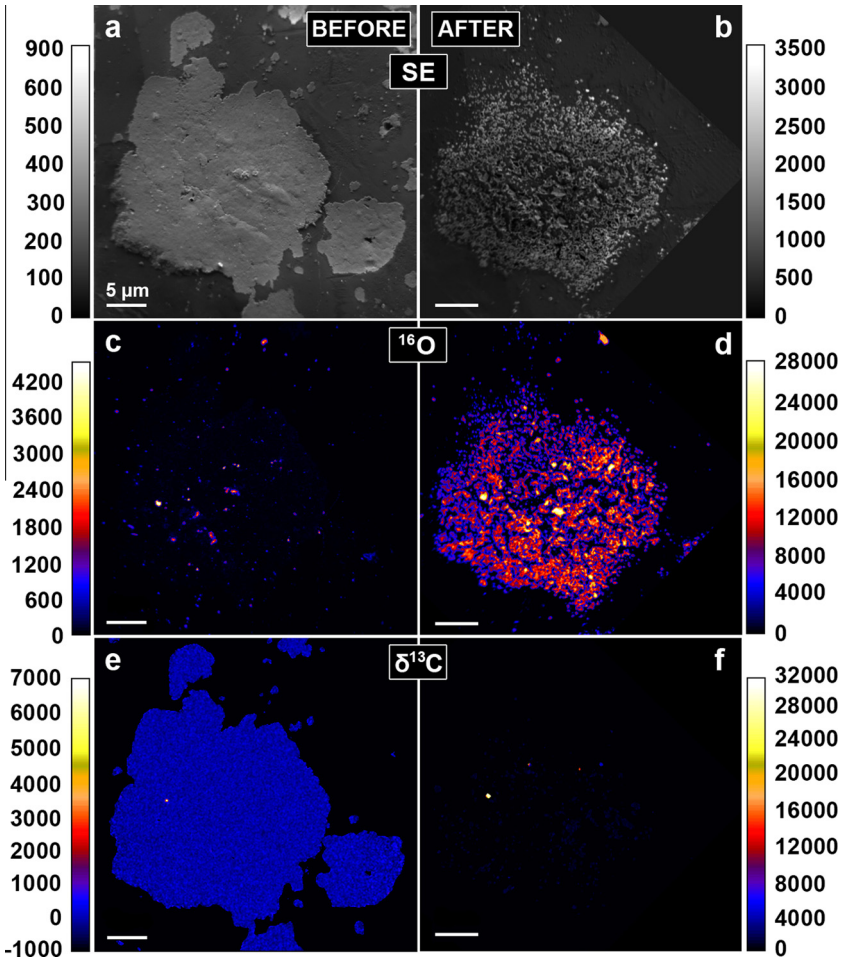

Fig. 2. NanoSIMS analysis comparison of MET 00426 (CR) IOM fragment #4 (a, c, e) before and (b, d, f) after the UV-ozone oxidation experiment. (a, b) Secondary electron images, (c,d) ^{16}O maps show the ozone oxidizes the IOM, and (e, f) $\delta^{13}C$ maps show how the same SiC grain has a different $\delta^{13}C$ value before (4900‰: $^{12}C/^{13}C = 15$; consistent throughout all 5 frames) and after oxidation of the IOM (31,000‰: $^{12}C/^{13}C = 3$; also consistent throughout all frames, i.e. SiC is not zoned). This shows that the IOM significantly dilutes the signal of the SiC grains. In some cases this could prevent the detection of SiC grains and thus abundances here should be considered as lower limits. The intensity scale corresponds to total number of counts with the exception of (e, f) which show $\delta^{13}C$ in per mil (‰). All scale bars are 5 µm.

to oxidation located 11 presolar SiC grains in ~3490 µm^2. Analysis after oxidation identified 41 in ~2760 µm^2. Not all pre-existing SiC grains could be relocated after oxidation, most likely because without IOM (which was probably located between the grains and sample substrate) adhesion is reduced resulting in the loss of SiC grains.

Presolar SiC grains measured post-oxidation possess a wider range of $^{12}C/^{13}C$ values (≈1–300; Fig. 3b) than seen prior to oxidation (~15–160; Fig. 3a). This is likely because many more grains were found after oxidation, increasing the probability that more isotopic variety would be present, and also because of dilution effects by the surrounding IOM. MET 00426 SiC grains found pre-oxidation had a median $^{12}C/^{13}C$ value of ~117, which is significantly higher than the ~53 ratio for post-oxidation grains that compares well to the ratio of ~50 to 56 determined for a large number of Murchison SiC grains from acid residues (e.g., Nittler and Alexander, 2003).

Two SiC grains, previously identified by NanoSIMS ion imaging, could be confidently relocated after removal of the surrounding IOM. The measured diameters of these increased from 380 nm to 540 nm, and from 330 nm to 480 nm, giving area increases of 100% and 110%, respectively (grains did not have perfectly circular surface areas). Post-oxidation grains are typically smaller (~230–550 nm in diameter; Fig. 3d and Table 2) than pre-oxidation grains (460–680 nm diameter; Fig. 3b; Table 2). Since IOM may partially mask the true SiC grain sizes, we would anticipate that grains would appear larger after removal of IOM. We would also expect that many smaller grains are entirely masked by IOM. It appears that the larger grains initially identified were most likely lost during mount handling after oxidation because the IOM adhered the SiC grains to the substrate. This is also supported by our inability to relocate most pre-oxidation SiC grains in areas where IOM was completely removed by oxidation. The high abundance of smaller grains after the removal of IOM is probably because they are initially entirely coated and embedded in the surrounding IOM with larger grains protruding from the IOM surface. Isotopic dilution from surrounding

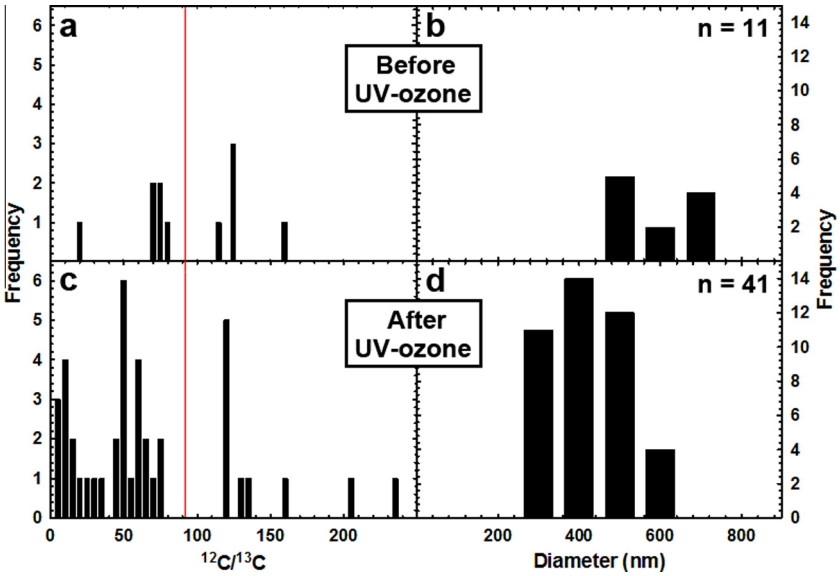

Fig. 3. (a, c) $^{12}C/^{13}C$ ratio distribution graphs (line = bulk IOM value of ~91; Alexander et al., 2007), and (b, d) size (diameter in nm) distribution graphs for all presolar SiC grains located in the IOM of MET 00426. (a, b) before and (c, d) after the UV-ozone oxidation experiment. The gap around the bulk IOM value show that presolar SiC grains with such "normal" isotopic compositions are not detected. Asymmetry of SiC $^{12}C/^{13}C$ ratios around the bulk IOM value is a function of frequency binning and the probability/difficulty of detecting a grain with low ^{13}C. *Y*-axis is frequency by number.

IOM in the NanoSIMS images will also preferentially mask smaller SiC grains. After the removal of the IOM, these smaller grains would be much more visible.

The oxidation of IOM samples is not helpful for the calculation of presolar grain abundances as the grains have been concentrated from an unknown initial volume of material and not a 2D plane of known dimensions (as with normal raster ion imaging of IOM). However, this technique could be useful for enriching samples in presolar SiC for further analysis.

3.4. SiC abundance uncertainties

SiC abundances derived for the various meteorites are given in Table 2. Column 8 gives the raw abundances derived from Eq. 1, with asymmetric 1–σ errors. These errors correspond to the uncertainty in the area fraction measurements (ν in Eq. 1) and are based solely on counting statistics (i.e., the number of identified presolar grains, after Gehrels, 1986). It may be possible to estimate more realistic errors for this term, also taking into account the measured grain sizes (R. Ogliore, pers. comm.), but we have chosen not to do so because the small-number statistics and systematic errors dominate the error budget. Furthermore, the lack of significant scatter in our abundance data suggests that the calculated errors are over-estimates. An additional random source of uncertainty arises from errors in the estimated matrix abundances ($\overline{Y}$ in Eq. 1) used to matrix-normalize SiC abundances. Finally, systematic bias is introduced by both (1) failure to detect grains either because their sizes were less than or equal to the primary beam diameter or because they are less isotopically anomalous (i.e., they did not satisfy the 3σ isotope anomaly criterion), and (2) underestimation or overestimation of grain sizes due to masking by IOM or potential preferential sputtering of IOM relative to SiC, respectively. Below we discuss our quantitative estimates for these additional sources of error (see also Table 2):

3.4.1. Errors in estimated matrix abundances

Matrix-normalization of abundances is used for two reasons: (a) to enable comparison with data reported in the literature (matrix values used for normalization are not always stated and thus it is not possible to convert matrix-normalized SiC abundances to bulk SiC abundances), and (b) because presolar SiC grains are found exclusively in the matrix and fine-grained chondrule rims of meteorites. Because matrix is present in meteorites in varying abundances, it is necessary to matrix-normalize in order to compare SiC abundances in the precursor material of each different meteorite/group. Multiple components contribute to the error for estimating matrix abundances: (i) errors introduced when determining the matrix volume for a particular thin section, (ii) differences between thin sections that arise from heterogeneous distribution of components throughout a meteorite (some meteorites show considerable variation in the area fraction of matrix between different thin sections; e.g., Weisberg et al., 1993; Schrader et al., 2011), (iii) different studies use different definitions of matrix, and (iv) primordial matrix can be difficult to identify in altered meteorites or those that are brecciated (such as many CMs). Our estimates of the contribution of the matrix abundance error to the total abundance error are given in Table 2 (column 11). Matrix abundances were taken from the literature (Weisberg et al., 1993; Alexander et al., 2007 and references therein; Davidson et al., 2009b; Schrader et al., 2011), and are generally considered to be accurate within 10%

(Schrader et al., 2011). Errors associated with matrix abundances were estimated here by calculating presolar SiC abundances using matrix abundances 10% either side of the quoted values (i.e., matrix abundance − 10% to matrix abundance + 10%).

3.4.2. Non-detection of small or less isotopically anomalous grains

Because grain size distributions appear to vary between meteorites, correcting for non-detection of small grains requires some prior knowledge of the true size distribution of grains (i.e., by another method, such as SEM analysis). However, because undetected grains are small, unless they are present in unrealistically high abundance, they have little effect on total SiC abundances. For example, if 10 grains ~100 nm in diameter (typical beam size) were missed for every 10 grains detected (i.e., a 50% detection efficiency) this would change abundances by only ~2% assuming a typical SiC size distribution (Amari et al., 1994).

Presolar SiC grains with approximately solar $^{12}C/^{13}C$ ratios (e.g., IOM-like $\delta^{13}C$ values typically between −6‰ and −26‰; Alexander et al., 2007) will not have been detected. The degree to which somewhat more anomalous grains were not detected will have been a function of the uncertainties in the C isotopic measurements (typically 5–10%). Isotopic dilution by surrounding IOM will also make some presolar grains, particularly small and less isotopically anomalous ones, undetectable, which may explain so-called "hotspots" in some $^{28}Si/^{12}C$ maps that are without correlated anomalies in the $^{13}C/^{12}C$ maps. However, it is not possible to determine if these hotspots are presolar SiC grains without extraction from the IOM and subsequent analysis. Small silicate grains have been found to occasionally survive IOM isolation and could also explain these $^{28}Si/^{12}C$ hotspots (Alexander et al., 2007). It is possible to estimate the number of undetected grains using two approaches. (1) When the grain size of detected grains is plotted against their $^{12}C/^{13}C$ ratios, it is possible to fill in the gap present around solar values assuming a distribution like that seen in isolated Murchison SiC grains (Amari et al., 1994). This leads to an estimated non-detection of only 5% of all grains. (2) The $^{12}C/^{13}C$ ratio distribution of data presented here can be approximately reproduced by mixing that of previously published data (presented as relative frequency of grains rather than total number of grains) with 50% isotopically normal C to simulate the effect that dilution by surrounding IOM has on the C-isotopic composition of SiC grains. Using this method to estimate missed grains also yields non-detection rates of ~5% of all grains.

3.4.3. Under- and over-estimates of grain size

Partial masking of grains by IOM in the NanoSIMS images could lead to an underestimate of their sizes. The areas of two grains confidently relocated after removal of surrounding IOM by UV-ozone oxidation increased by 100% and 110%, respectively. Thus, partial masking of the SiC by IOM could lead to inferred bulk SiC abundances that are roughly half of the actual abundances. However, this estimate is based on only two examples and thus has not been applied here. This issue can only be addressed in a dedicated study applying the same experimental methods on both IOM and bulk material extracted from the same meteoritic sample. Another potential bias would arise if IOM sputters significantly faster than SiC, as the SiC area fraction would become larger as grains are excavated, leading to an overestimate of grain sizes. However, high-resolution field emission SEM imaging after NanoSIMS analysis showed that there was no appreciable height difference between the grains and surrounding IOM (Davidson, 2009). Thus, there is no evidence for preferential sputtering. Results from the oxidation experiment suggest that, if anything, grain sizes are consistently underestimated when analyzed in an IOM substrate.

The non-detection of small or isotopically normal grains, and underestimates of grain sizes discussed above both lead to underestimates of reported grain abundances and we thus apply positive corrections to our abundance estimates, based on the above discussions (columns 9 and 10 of Table 2). Column 13 of Table 2 gives the final corrected SiC abundances with uncertainties based on combining in quadrature the counting statistics error and the error in the matrix fraction of each meteorite. Note that these errors may be overestimates as the data cluster more closely than the final errors suggest that they should. The mean and standard deviation of the abundances of all CR chondrites may provide a more accurate estimated degree of error.

3.5. Presolar SiC abundances

SiC abundance results for the 14 meteorites, including the uncertainties as discussed above, are detailed in Table 2 and shown in Fig. 4. The CI Orgueil gave a matrix-normalized abundance of 34^{+11}_{-8} ppm; considerably larger than the 14.2 ± 1.9 ppm previously determined using noble gas tracer abundances (assuming a "constant" noble gas component Ne-E(H) concentration) in acid residues (Huss and Lewis, 1995), but comparable to the 28.5 ± 5.6 ppm abundance calculated using "variable" Ne-E(H) concentrations (where one of five values for Ne-E(H) content of SiC was used depending on the Ne-E(H)/Xe-S(H) in the sample; see Table 17 of Huss and Lewis (1995) and discussion therein).

Our Murchison (CM2) SiC abundance of 14^{+4}_{-3} ppm is lower than the 21.2 ± 2.2 ppm obtained by Huss et al. (2003) from noble gases. Both values are lower than the value of 35^{+16}_{-12} ppm determined for Bells (which may result from the presence of unusually large grains). However, the CM group average of 21 ± 5 ppm determined here agrees with the abundance determined by noble gas analysis for Murchison.

Presolar SiC abundances for the seven CR chondrites measured here vary from 24^{+5}_{-5} ppm (GRO 95577) to 47^{+18}_{-14} ppm (EET 92042) with an average of 32 ± 9 ppm. The abundances determined here by NanoSIMS are significantly higher than those determined from noble gases for Renazzo. Our calculated Renazzo abundance of 35^{+14}_{-11} ppm is ~20 times larger than the 1.8 ± 0.6 ppm determined from noble gases (1.6 ± 0.6 ppm using the same matrix abundance

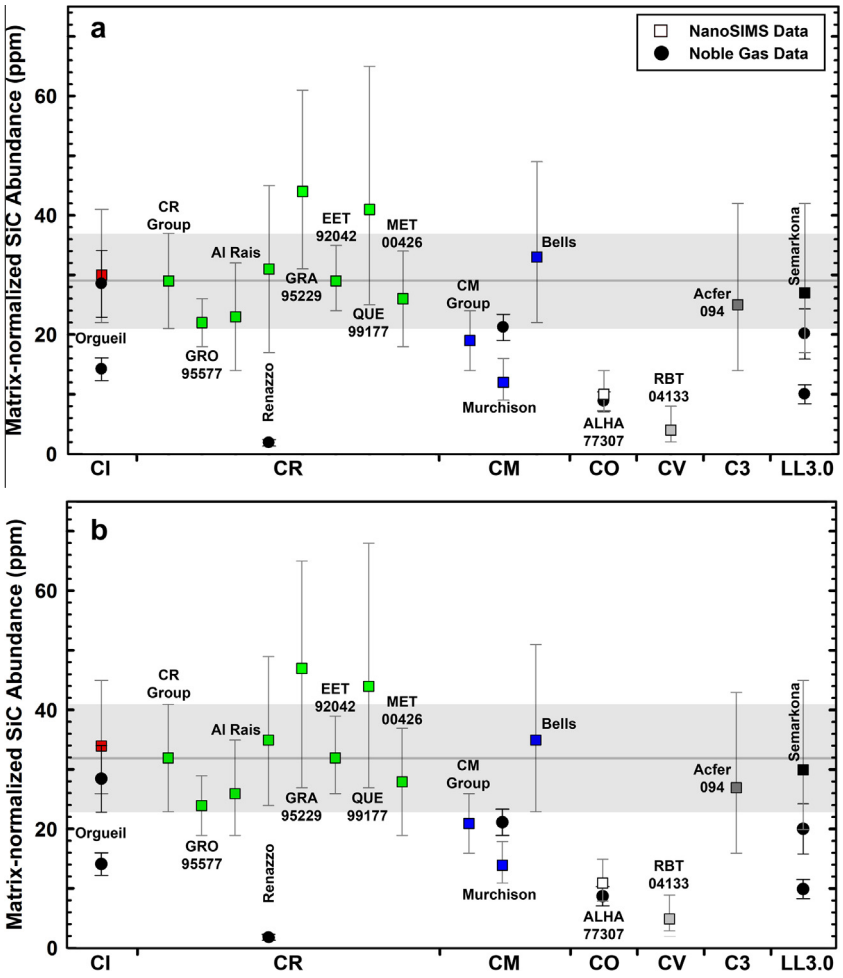

Fig. 4. (a) Uncorrected, and (b) corrected matrix-normalized presolar SiC abundances (ppm) in primitive chondrites analyzed here with NanoSIMS and by noble gas analyses (Huss and Lewis, 1995; Huss et al., 2003; two data points for Orgueil and Semarkona reflect constant and variable Ne-E(H) contents as discussed in the main text). Order (left-to-right) corresponds to the order in Table 2 (top-to-bottom). CR chondrite group mean (grey line) and one standard deviation range (light grey shading) are shown for comparison.

as this work; Huss et al., 2003), and also in agreement with 50^{+90}_{-30} and 55^{+53}_{-30} ppm determined by the *in situ* matrix studies of Floss and Stadermann (2005) and Leitner et al. (2012a), respectively. Our abundance for GRA 95229 (47^{+18}_{-14} ppm) agrees with 57^{+45}_{-27} ppm determined by an *in situ* matrix study (Leitner et al., 2012a). Similarly, our abundance for QUE 99177 (44^{+24}_{-17} ppm) agrees with higher abundances from *in situ* matrix measurements of $\sim 45^{+14}_{-11}$ and 55^{+20}_{-15} ppm reported by Floss and Stadermann (2009a) and Nguyen et al. (2010), respectively. The uncertainties in the *in situ* measurements were re-calculated in the same manner as those reported for analyses here (i.e., based on counting statistics; Gehrels, 1986). Significantly higher presolar SiC grain abundances have been reported from *in situ* matrix studies of other CR chondrites NWA 852 (160 ± 57 ppm; Leitner et al., 2012c) and GRV 021710 (182 ± 33 ppm; Zhao et al., 2013).

RBT 04133 (reduced CV3.4) has a presolar SiC abundance of only 5^{+4}_{-2} ppm; Huss and Lewis (1995) and Huss et al. (2003) also reported low SiC abundances of ~0.48–1.1 ppm for reduced CV3 chondrites. The CO3.0 ALHA 77307 has a matrix-normalized presolar SiC abundance of 11^{+4}_{-3} ppm; this agrees with the 8.8 ± 1.6 ppm reported by Huss et al. (2003), but is much lower than the 110 ± 20 ppm reported from *in situ* measurements (Bose et al., 2012). Acfer 094 (ung. C3) yielded an abundance of 27^{+17}_{-11} ppm, which agrees with 29 ± 6 ppm calculated from stepped combustion analyses (Newton et al., 1995) and is within error of the 11–17 ppm abundance for presolar SiC calculated by combined SEM/ion probe measurements of a SiC/spinel residue (Gao et al., 1996). The only ordinary chondrite studied here, LL3.0 Semarkona, yielded a presolar SiC abundance of 30^{+15}_{-10} ppm, which is 3 times larger than the 10.0 ± 1.6 ppm determined from noble gas analyses using constant Ne-E(H), but is comparable, within error, to the 20.1 ± 4.2 ppm determined using variable Ne-E(H) (Huss and Lewis, 1995).

3.6. Presolar SiC $^{12}C/^{13}C$ ratio distributions

As confirmed by the oxidation experiment, some dilution of the $^{12}C/^{13}C$ ratios of SiC grains is expected as a

result of overlap of the SIMS primary ion beam with the surrounding IOM. This dilution should shift the measured $^{12}C/^{13}C$ ratios towards the solar (89) and bulk IOM (~91) values and will result in lower detection efficiencies of small and/or ^{13}C-poor grains. The median $^{12}C/^{13}C$ ratio of 71 for all 177 grains (114 for all CR chondrite SiC grains; excluding MET 00426 post-oxidation [PO] grains) is higher than the values reported for Murchison; Nittler and Alexander (2003) found a median ratio of 56 for previously published Murchison data, and a ratio of ~50 for the ~3300 SiC grains found in their study of Murchison residues. Both these Murchison ratios agree with the median ratio of ~53 calculated for the 41 post-oxidation MET 00426 grains (the median ratio was ~117 prior to oxidation, albeit for a smaller number of grains). Indeed, the $^{12}C/^{13}C$ ratio distribution of data presented here can be reproduced by mixing previously published data with 50% isotopically normal C to simulate dilution. Therefore, this dilution effect should be borne in mind during the following discussion.

The $^{12}C/^{13}C$ ratios of isolated presolar SiC grains (Fig. 5) span a very wide range, but show a strong peak at a value of ~60 (see, e.g., Murchison example Fig. 5f;

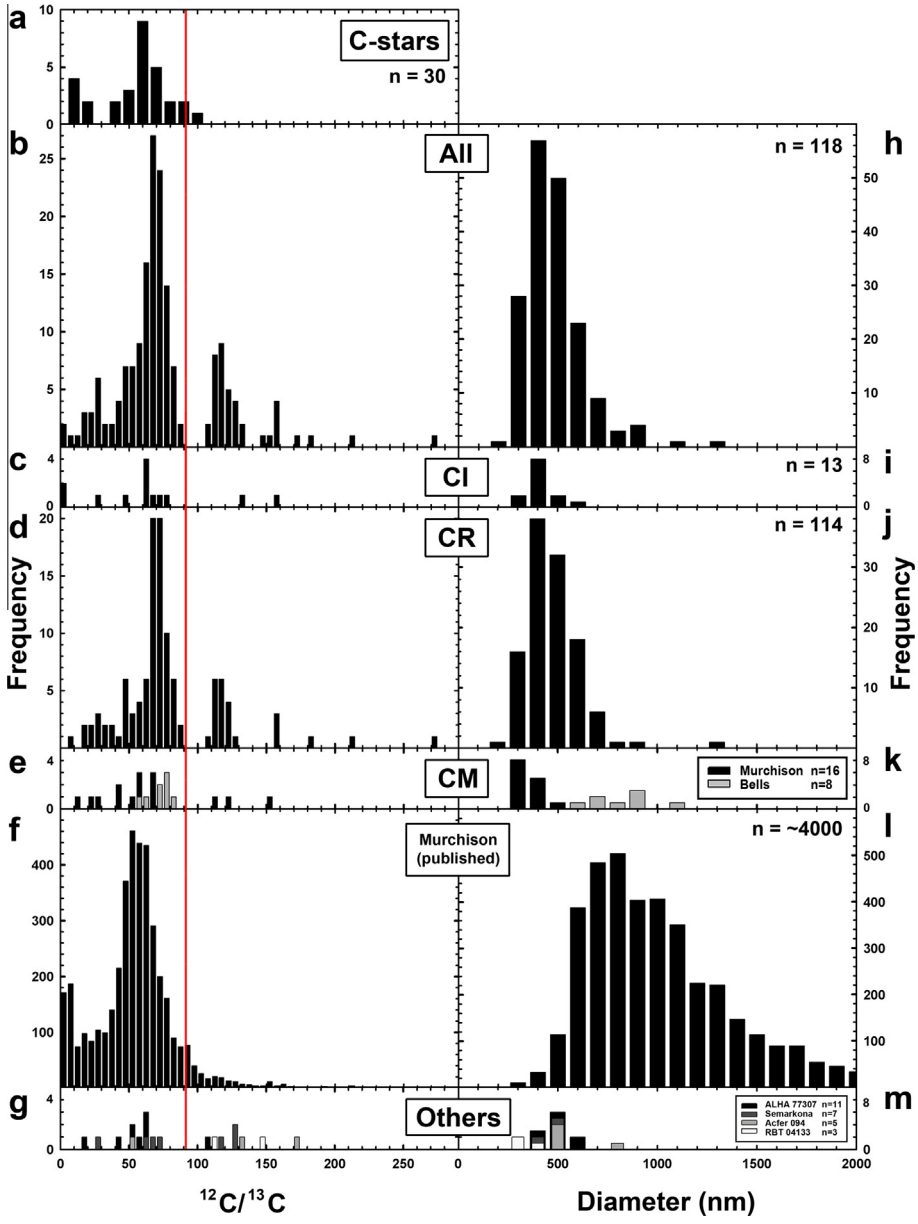

Fig. 5. (a–g) $^{12}C/^{13}C$ ratios (left) and (h–m) size distributions (right) for all presolar SiC grains located in the IOM of the primitive chondrites studied here (line = bulk IOM value of ~91; Alexander et al., 2007), (a) carbon stars (data from Lambert et al., 1986), and (f, l) published data for CM2 Murchison (Hynes and Gyngard, 2009, and references therein; NB. grains in the Presolar Grain Database are biased towards larger grain sizes). Size is grain diameter in nanometers. *Y*-axes are frequency by number. Figure does not include post-oxidation data for MET 00426. Asymmetry of SiC $^{12}C/^{13}C$ ratios around the bulk IOM value is a function of frequency binning and the probability/difficulty of detecting a grain with low ^{13}C.

Alexander, 1993; Hoppe et al., 1994; Nittler and Alexander, 2003; Hynes and Gyngard, 2009) in good agreement with astronomical measurements of C stars (Fig. 5a; Lambert et al., 1986). All meteorites studied here have similar distributions, with the exception of RBT 04133 (which is likely due to the low number of grains present in this sample) and MET 00426. The only three grains from RBT 04133 (CV3) have ratios of around ~120, showing neither extremely ^{12}C-poor nor ^{12}C-rich grains (Fig. 5g). MET 00426 shows a larger than typical fraction of grains with ^{12}C/^{13}C ratios higher than solar (compare to Fig. 5b), especially before UV-ozone treatment (Fig. 3); this is likely a statistical effect. Not all samples show the wide range of values seen in Murchison data from the Presolar Grain Database (Fig. 5f; Hynes and Gyngard, 2009; and references therein), but this is likely due to overlap with IOM and the smaller sample sizes in this study.

3.7. Presolar SiC size distributions

Although the oxidation experiment showed that overlap by IOM will lead to an underestimate of SiC grain sizes, it is still possible to qualitatively compare grain sizes between samples, as they will all be underestimated to similar extents. The size distributions of the presolar SiC grains located in this study show some variation between chondrite groups. The size distributions of presolar SiC grains from the CR chondrites (Fig. 5j) agree well within the group (Table 2; means of ~400–500 nm diameter) and with the CI Orgueil (Fig. 5i). The Murchison grains identified here are entirely ⩽500 nm in diameter (Fig. 5k). Bells has the coarsest-grained SiC of all the measured samples (Fig. 5k; 770 nm mean diameter; Table 2).

The size distributions of presolar SiC grains from ALHA 77307, Acfer 094, and Semarkona are similar to one another (Fig. 5m; Table 2). On the basis of the average diameters, Acfer 094 SiC is slightly coarser-grained than that in all other groups except the CM chondrites (Table 2). ALHA 77307 grains show limited variation in diameters, but peak at the same size as other samples. RBT 04133 may be finer-grained than most other samples, being dominated by grains ~300 nm in diameter, but the sample size of three grains is too small to be conclusive.

4. DISCUSSION

4.1. Presolar SiC abundances determined by NanoSIMS vs. noble gas analyses

The SiC abundances determined here by NanoSIMS are compared to those from noble gas analysis (Huss and Lewis, 1995; Huss et al., 2003) in Figs. 4 and 6. There are systematic disagreements between the abundances determined by NanoSIMS and by noble gas analyses based on constant Ne-E(H) for Orgueil (CI), Renazzo (CR), and Semarkona (LL) (the noble gas data give ~15–30 ppm lower SiC abundances; Fig. 6). However, the Orgueil and Semarkona data agree when variable Ne-E(H) is used to calculate SiC abundances via the noble gas method. The presolar SiC abundance of the only CI studied here

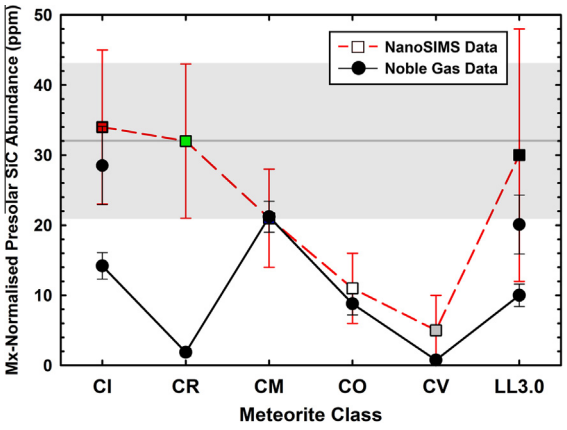

Fig. 6. Matrix-normalized presolar SiC abundances determined by NanoSIMS ion imaging (this work) and from their exotic noble gas components (Huss and Lewis, 1994, 1995; Huss et al., 1996, 2003; two data points for Orgueil and Semarkona reflect constant and variable Ne-E(H) contents as discussed in the main text). CR chondrite group mean (grey line) and one standard deviation range (light grey shading), 32 ± 9 ppm, are shown for comparison.

(Orgueil; 34^{+11}_{-8} ppm) is in agreement with the matrix-normalized CR chondrite SiC abundances measured here (32 ± 9 ppm group average), which confirms that the CR chondrites have higher, more CI-like SiC abundances than previously believed (e.g., Huss and Lewis, 1995; Huss et al., 2003). Our conclusion, that CR chondrites have higher presolar SiC abundances than previously reported via noble gas analysis, is supported by similar or higher abundances (up to ~100 ppm or more) from *in situ* ion imaging studies (Floss and Stadermann, 2005, 2009a; Nguyen et al., 2010; Leitner et al., 2012a,c; Zhao et al., 2013, see discussion below).

There is agreement between presolar SiC abundances for the CM average and ALHA 77307, and also Orgueil and Semarkona determined here and those based on noble gases, when abundances are calculated using variable Ne-E(H) (Figs. 4 and 6; Table 2; Huss and Lewis, 1994, 1995; Huss et al., 1996, 2003). It is highly unlikely that these agreements are statistical flukes. It is more likely that the agreement found for these samples, but not for CR chondrites, is because the SiC grains in these samples were not subjected to the same parent body processes as the CR chondrites.

There are several possible explanations for differences in presolar SiC abundances estimated by NanoSIMS and those by noble gas analyses: (1) effects of laboratory processing, (2) addition of a noble gas-free SiC component to some meteorite-forming regions, (3) size-dependence of noble gas abundances in SiC grains and variable size distributions between chondrite groups, and (4) loss of a major fraction of the noble gases from SiC grains in some meteorite groups (either in the nebula or on the parent body).

(1) *Effects of laboratory processing*. Multiple lines of evidence suggest that laboratory processing of IOM is not responsible for the varying abundances seen, including; (i) the agreement between SiC abundances determined from Murchison A and B residues that

were prepared by different techniques, (ii) the different SiC abundances in residues from different meteorites prepared in the same way, (iii) the agreement between SiC abundances measured on microtomed and non-microtomed samples, and (iv) the agreements found by NanoSIMS and noble gas analyses for presolar SiC abundances in the CMs, ALHA 77307, and Semarkona.

(2) *Addition of a noble gas-free SiC component*. If addition of gas-free SiC is the explanation for the differences in SiC abundances between those measured here and those estimated from noble gases, this gas-free SiC would have to have been added between the time of formation of the CI-CM-OC/Acfer 094 chondrites and that of the CRs. One way to introduce additional grains into the forming Solar System would be the injection of material from a nearby supernova event (e.g., Nittler et al., 2008; Qin et al., 2011). However, this injection of supernova material would mean that the added gas-free SiC grains were supernova grains (i.e., of types X and C; Zinner, 2014 and references therein). The abundance of such grains is both low (~1% of all SiC grains) and similar across different classes of carbonaceous chondrites (e.g., Hynes and Gyngard, 2009 and references therein) and the grains have significantly different C- and N-isotopic distributions. The C- and N-isotopic compositions of the CR grains located here are similar to those of the other meteorite groups and indicate that their sources are dominantly Asymptotic Giant Branch (AGB) stars (Zinner, 2014 and references therein), not supernovae.

(3) *Grain-size-dependence of noble gas abundances*. The abundances of presolar SiC grains estimated by noble gas analyses are based on the Ne-E(H) (now also known as Ne-R) content of Murchison SiC determined by Lewis et al. (1994). However, the absolute and relative concentrations of the Ne-E(H) and Xe-S components in Murchison SiC vary with grain size (Lewis et al., 1994); Ne-E(H) concentrations increase and Xe-S concentrations decrease with increasing grain size. Russell et al. (1997) found that the fine-grained SiC in the enstatite chondrite Indarch (EH4) has a lower Ne-E(H)/Xe-S ratio than the coarser-grained SiC in Murchison, showing that the ratio is indeed size-dependent. The grain size variations in absolute and relative noble gas abundances probably largely reflect the implantation depths of the noble gas components into the SiC (Alexander, 1994; Verchovsky et al., 2004). Thus, either the loss of presolar SiC grains within a particular size range, or the removal of the presumably damaged and gas-rich outer portions of the SiC would reduce the absolute noble gas abundances and change the Ne-E(H)/Xe-S ratios determined for any given meteorite. The meteorites analyzed here by NanoSIMS with finer-grained SiC (e.g., Orgueil, the CR chondrites, and Semarkona) should have low Ne-E(H)/Xe-S ratios which is the case at least for Orgueil and Semarkona (Russell et al. 1997, and references therein). As the Ne-E(H)/Xe-S ratio is size-dependent, estimating SiC abundances using constant concentrations of Ne-E(H) determined from coarse-grained Murchison SiC will lead to inaccurate determinations of abundances by up to a factor of two for some meteorites, depending on whether their presolar SiC is finer- or coarser-grained (Huss and Lewis, 1995). Consequently, the fine-grained meteorites (Orgueil, the CR chondrites, and Semarkona) will have higher SiC abundances when determined by NanoSIMS than by noble gas analyses. Indeed, differences vary by ~15–30 ppm (Fig. 6), and all plot close to CI abundance on the basis of the NanoSIMS data from this study. Furthermore, presolar SiC abundances for Orgueil and Semarkona determined using variable Ne-E(H) concentrations (Huss et al., 1995) are in agreement with those determined by NanoSIMS ion imaging here. Therefore, differences between presolar SiC abundances determined by noble gas analysis and NanoSIMS ion imaging for some meteorites (i.e., Orgueil and Semarkona) can be satisfactorily explained as resulting from the heterogeneous distribution of Ne-E(H) in SiC grains of different sizes. However, this is not sufficient to explain the dramatic difference in presolar SiC abundances determined for the CR chondrite Renazzo by the two techniques.

(4) *Noble gas loss from SiC*. The temperatures required to degas SiC are lower (400–450 °C; Huss et al., 2003) than those required for destruction in the nebula (based on stepped-combustion experiments; ~550 °C for finest-grained SiC; up to ~1300 °C for largest grains and aggregates; Russell et al., 1997). The CR IOM is primitive in nature and experienced peak temperatures of <240 °C (Busemann et al., 2007; Cody et al., 2008), which is not high enough to degas or destroy SiC grains, at least via purely thermal alteration. Partial destruction resulting in gas loss of SiC in the nebula is probably controlled by diffusion rates through a surface oxide layer. In contrast, in a parent body setting, over longer timescales with a means to diffuse silica away from the grain surface and in the presence of an oxidant, the temperature required for at least partial degassing may have been much lower than 400 °C (Alexander et al., 1990a). The CR chondrites exhibit a range of aqueous alteration (Weisberg et al., 1993). While similar presolar SiC abundances for CR3s to CR1s indicate that increasing aqueous alteration did not progressively destroy SiC grains in the CR parent body, degassing of SiC may have occurred during alteration; SiC grains may have formed an outer layer of SiO_2 that was not thermodynamically stable and reacted to form clays. Phyllosilicates have been identified in all CRs (Weisberg et al., 1993), including those argued to be CR3s (Abreu and Brearley, 2010). Alternatively, some presolar SiC could have been degassed prior to accretion. This would require that the IOM was mixed into the matrix material

later to escape this heating. This seems unlikely because of the well-mixed presence of both components in the matrix. The sustained heating necessary to degas SiC in the nebula may have modified the microstructure of some matrix silicates, such as recrystallizing amorphous material. However, abundant amorphous material is present in the matrices of the most primitive CRs (Abreu and Brearley, 2010).

In conclusion, data obtained here by direct ion imaging are more robust than previous estimates based on the detection of noble gases. The abundances determined here can now be meaningfully compared amongst and between groups in order to investigate the variable evolution and processing experienced by the different chondrite classes.

4.2. Presolar SiC abundances determined by ion imaging of IOM residues vs. *in situ* matrix abundances

Some presolar SiC abundances determined by *in situ* ion imaging studies (e.g., Floss and Stadermann, 2009a; Bose et al., 2012; Leitner et al., 2012c; Zhao et al., 2013) are substantially higher (up to ~100 ppm) than those determined by ion imaging of IOM residues here (e.g., CR group average: 32 ± 9 ppm). In order to meaningfully compare abundances determined by the two different techniques, the uncertainties in the *in situ* measurements were re-calculated in the same manner as those reported for analyses here (i.e., based on counting statistics; Gehrels, 1986). Errors determined by this method are larger than those reported in the original studies. Presolar SiC abundances from *in situ* studies range from 45^{+14}_{-11}–55^{+20}_{-15} ppm (QUE 99177; Floss and Stadermann, 2009a; Nguyen et al., 2010), 50^{+90}_{-30} 55^{+53}_{-30} ppm (Renazzo; Floss and Stadermann, 2005; Leitner et al., 2012a), 57^{+45}_{-27} ppm (GRA 95229; Leitner et al., 2012a), 90^{+22}_{-18} ppm (MET 00426; Floss and Stadermann, 2009a), 110^{+27}_{-22} ppm (ALHA 77307; Bose et al., 2012), 160^{+90}_{-30} ppm (NWA 852; Leitner et al., 2012c), to 182^{+45}_{-27} ppm (GRV 021710; Zhao et al., 2013). The differences between the *in situ* measurements and our IOM study may result from the destruction or loss of SiC grains during IOM residue preparation, presence of unusually large SiC grains in some *in situ* studies, unrealistically low associated errors, sample heterogeneity, and/or a lower detection efficiency for presolar SiC grains in a carbonaceous matrix (this work) compared to an O-rich matrix (*in situ* studies). The destruction of SiC grains during IOM residue preparation cannot be ruled out. However the smaller grains are likely to be destroyed and, as previously discussed, they do not significantly affect abundances. The presolar SiC abundance for the CR chondrite GRV 021710 (28 SiC grains) is dominated by a single grain (1060×800 nm diameter); if the largest grain is omitted, the abundance drops from 182^{+41}_{-34} ppm to 120^{+28}_{-23} ppm. As the abundance is heavily dependent on a single grain, the reported abundance error of only ±33 ppm (Zhao et al., 2013) appears to be under-estimated.

Clustering of presolar silicate grains (i.e., sample heterogeneity at tens to hundreds of micrometer scales) has been reported in *in situ* matrix studies of various carbonaceous chondrites (e.g., Davidson, 2009; Vollmer et al., 2009; Floss and Stadermann, 2009b) and IDPs (Busemann et al., 2009; Davidson et al., 2012b). No apparent heterogeneity was observed in NWA 852 (Leitner et al., 2012c).

Possibly the differences can be explained largely by sample heterogeneity at a sub-mg/sub-mm scale. Presolar grains are heterogeneously distributed in matrix (e.g., Davidson, 2009; Vollmer et al., 2009; Floss and Stadermann, 2009b) and IDPs (e.g., Busemann et al., 2009; Davidson et al., 2012b). Results of *in situ* studies are also heavily dependent on which areas are selected for mapping. For example, *in situ* studies of matrix may focus on sub-areas that have been previously identified as having high presolar grain concentrations, as was the case for ALHA 77307 (Bose et al., 2012). Studies of presolar SiC abundances determined from raster ion imaging of IOM residues are less affected by such heterogeneity as they are more representative of bulk material (residues are prepared from gram-sized samples that were thoroughly mixed during processing). Thus, it is possible that the apparent discrepancies between abundances from ion imaging of matrix *in situ* and IOM result largely from sample heterogeneity. Regardless, CR chondrite SiC abundances determined by both ion imaging techniques are significantly higher than those determined by noble gas analyses.

4.3. Presolar SiC: abundance variations between meteorite groups

The matrix-normalized presolar SiC abundance for Murchison determined here by NanoSIMS ion imaging of IOM is lower than found for the CI chondrites, suggesting that Murchison is not as pristine as originally believed. The CR chondrites (32 ± 9 ppm) are closer to the CIs in terms of presolar SiC abundances than previously determined on the basis of noble gas analyses alone (Renazzo; 1.86 ± 0.55 ppm; Huss et al., 2003), and are roughly in concordance with the even slightly higher abundances reported by some *in situ* studies of CR chondrites (e.g., Floss and Stadermann, 2005, 2009a; Nguyen et al., 2010, but see also above). Having ruled out the effects of laboratory processing (Section 4.1), there are three possible explanations for the variations in presolar SiC abundances seen between meteorite groups: (1) terrestrial alteration, (2) pre-accretion heterogeneities in the solar nebula, or (3) alteration in the parent body.

(1) *Terrestrial alteration*. Al Rais and Renazzo are falls; all other CR chondrites studied here are Antarctic finds. Our NanoSIMS-determined presolar SiC abundances of the falls Al Rais (CR2, revised compared with Davidson et al., 2008) and Renazzo agree well with the other CR chondrites, demonstrating that Antarctic weathering of a meteorite does not affect its presolar SiC abundance.
(2) *Pre-accretion heterogeneities (nebular processes)*. The varying presolar SiC abundances seen between different meteorite groups could be explained by the loss of presolar SiC prior to accretion (e.g., Huss et al.,

2003). The CI chondrites and groups with CI-like presolar SiC abundances (i.e., all samples studied except ALH 77307, RBT 04133 and Murchison) suggest a homogeneous SiC abundance in the nebula. However, the difference seen in presolar SiC abundances estimated here by NanoSIMS ion imaging for Murchison (14^{+4}_{-3} ppm) compared with the CR chondrites (32 ± 9 ppm), CI Orgueil (34^{+11}_{-8} ppm), LL Semarkona (30^{+15}_{-10} ppm) and ungrouped C3 Acfer 094 (27^{+17}_{-11} ppm) represents a ~50% loss of SiC in Murchison relative to the CR/CI/LL/Acfer 094/Bells chondrites. Aerodynamic size-sorting of early Solar System materials during their fall through solar nebula gas toward the proto-Sun has been suggested to explain the differing size distributions of chondrules, CAIs and metal grains between meteorite groups (e.g., Scott and Haack, 1993; Kuebler et al., 1999). However, the size-sorting process for SiC grains would have to have been different than that for chondrules as the sorting of chondrule-sized objects would remove all of the SiC. If size-sorting of presolar SiC grains did occur, it is likely that other presolar grains, such as nanodiamonds, would also have been affected (Russell et al., 1997). However, Russell et al. (1997) reported that there was no correlation seen between presolar SiC and nanodiamond abundances. Since nanodiamonds are entirely 1 to 5 nm in diameter, they should be completely removed with finer-grained SiC (Russell et al., 1997) unless they are present as larger aggregates. Thus, these contradictory observations imply that pre-accretionary size-sorting is an unlikely explanation for the variability in presolar SiC abundances seen here.

(3) *Parent body alteration*. RBT 04133 (CV3), which has a very low matrix-normalized SiC abundance of 5^{+4}_{-2} ppm, shows evidence for heating in its parent body at ~440 °C (Davidson et al., 2009b), sufficient to explain the destruction of presolar SiC in this meteorite. However, more prolonged, low-temperature alteration would be required to significantly affect the SiC abundances in the majority of the meteorites analyzed here, as they have not experienced such high temperatures. Similar presolar SiC abundances for CR chondrites of different petrographic type (CR3 to CR1) show that increasing degrees of aqueous alteration in the CR parent body did not progressively destroy SiC under the conditions at which the CR chondrites were altered (8–43 °C; Guo, 2009). However, it is possible that the outer noble-gas-rich portions of the grains were destroyed (Section 4.1). The CM Murchison was subjected to estimated peak temperatures of ~20–33 °C (Clayton and Mayeda, 1984; Zolensky et al., 1997; Baker et al., 2002; Guo and Eiler, 2007). These temperatures are estimated from the formation temperature of carbonate (Guo and Eiler, 2007) and the assumption that alteration occurred under O-isotopic equilibrium (Clayton and Mayeda, 1984), which is unlikely. Therefore, it is possible that Murchison was subjected to slightly higher temperatures in its parent body. Indeed, this possibility has been suggested on the basis of the microstructure of IOM in Murchison and the other CMs (Alexander et al., in press). However, it is unlikely that they would be high enough to remove SiC by purely thermally-driven destruction. As previously discussed, it may be possible to degas/destroy SiC grains by prolonged parent body oxidation at low temperature; outer layers of thermodynamically unstable SiO_2 formed by oxidation of SiC dissolve to form clays. In the case of the CR chondrites, our SiC abundances combined with the noble gas data appear to require the degassing of SiC grains rather than their destruction. However, under the conditions experienced by the CM chondrites, which may have been more prolonged than those of the CR chondrites, destruction of smaller grains may have occurred by oxidation. Similarly, ALHA 77307 (CO3.0) has a low SiC abundance of 11^{+4}_{-3} ppm (but see also discussion of higher abundances from an *in situ* study above), and shows evidence for having experienced higher-temperature alteration than Semarkona (Busemann et al., 2007). Therefore, it is possible that processing in the parent body resulted in lower abundances in Murchison, ALHA 77307, and RBT 04133 compared to the CI, CR and LL chondrites, Acfer 094 and Bells.

If Bells is truly a CM chondrite, its isotopically anomalous IOM (Alexander et al., 2007) and the high SiC abundance determined here indicate that it is more primitive than other CM chondrites, such as Murchison. This is consistent with estimates of the extent of alteration based on water content (Alexander et al., 2013) and the low abundance of phyllosilicates determined from X-ray diffraction data (Howard and Alexander, 2013). However, the high SiC abundance in Bells may be a statistical fluke as a result of finding a low number of particularly large grains. Alternatively, this high abundance may indicate either heterogeneous accretion of the CM parent body or the action of some unidentified parent body process.

5. SUMMARY

1. We have measured presolar SiC abundances in IOM residues of primitive meteorites using NanoSIMS raster ion imaging, independently of noble gas analyses. Ion imaging is a direct technique, eliminating the uncertainties in the SiC abundances arising from noble gas analyses such as the size bias of noble gas concentrations (Huss and Lewis, 1995).
2. Whilst presolar SiC abundances obtained here with NanoSIMS for the CMs and ALHA 77307 (CO), and Orgueil (CI) and Semarkona (LL3.0) agree with data obtained by noble gas analyses (Huss et al., 2003) when variable Ne-E(H) concentrations are assumed, the values for Renazzo (CR) do not (Figs. 4 and 6; Table 2; Huss et al., 2003). Abundances estimated here for these

meteorites are similar/close to CI-like abundances and are roughly in concordance with, but lower than some, *in situ* observations of higher abundances for CR chondrites (Floss and Stadermann, 2005, 2009a; Nguyen et al., 2010; Leitner et al., 2012a,c; Zhao et al., 2013), whereas noble gas examinations suggest lower SiC abundances. Our revised higher value for CR chondrites is in agreement with observations that they are amongst the most primitive chondrites in terms of the isotopic compositions and disordered nature of their organic matter (e.g., Busemann et al., 2006, 2007; Alexander et al., 2007). Generally, we found in this NanoSIMS study of meteoritic IOM remarkably consistent presolar SiC abundances for primitive meteorites that have not undergone extensive parent body alteration from various classes (Fig. 4). This suggests the presence of a rather homogeneous mixture of presolar grains, organic matter and other matrix constituents in the meteorite-forming regions of the solar system. Potential inconsistencies with higher SiC abundances found *in situ* by NanoSIMS will have to be addressed in detail in a future study.

3. Discrepancies with abundances determined by noble gases (Huss and Lewis, 1995; Huss et al., 2003) indicate that the size-dependence of the concentrations (parameterized by Ne-E(H)/Xe-S) have to be considered. Nevertheless, the particularly low SiC abundance determined with noble gas concentrations for CR2 Renazzo remains enigmatic and may be explained by the loss of the outer noble gas-rich layers of SiC during low-temperature parent body oxidation.
4. Variations in SiC abundances between meteorite groups can be attributed to parent body alteration of an initial reservoir of homogeneous SiC abundances incorporated from the solar nebula. Thermal processing is capable of destroying SiC grains and, in the case of RBT 04133 (with an estimated peak metamorphic temperature of ~440 °C; Davidson et al., 2009b), led to a low abundance. However, not all meteorites experienced significant heating and similar SiC abundances in CR1, CR2 and CR3 chondrites confirm that SiC was not progressively destroyed by increasing degrees of aqueous alteration on the CR parent body. Thus SiC grain destruction must be explained by prolonged, low-temperature parent body alteration in the presence of an oxidant.

ACKNOWLEDGEMENTS

The authors would like to thank ANSMET, JSC, and MWG for providing the Antarctic meteorite samples, and Tim McCoy and Linda Welzenbach (USNM), Lora Bleacher (ASU) and Ansgar Greshake (MNB Berlin) for providing the non-Antarctic samples. This manuscript was significantly improved by helpful reviews from Yunbin Guan and an anonymous reviewer, and the editorial expertise of AE Anders Meibom. The authors would also like to thank Devin Schrader for helpful discussions and for providing additional matrix abundance data, and Ryan Ogliore for helpful discussions regarding error analysis. Funding from STFC is gratefully acknowledged for the Ph.D. studentship that supported this research (J.D.), the Aurora and advanced fellowship program (H.B.), and for the UKCAN facilities employed throughout this work. This work was supported in part by NASA Grants NNX10AI63G and NNX11AB40G to L.R.N.

REFERENCES

Abreu N. M. (2007) Fine-scale mineralogical study of the matrices of CR carbonaceous chondrites: insights on early Solar System processes. Ph. D. thesis, The University of New Mexico. pp. 224.

Abreu N. M. and Brearley A. J. (2010) Early solar system processes recorded in the matrices of two highly pristine CR3 carbonaceous chondrites, MET 00426 and QUE 99177. *Geochim. Cosmochim. Acta* **74**, 1146–1171.

Alexander C. M. O'D. (1989) The microstructure of Semarkona and Bishunpur. *Geochim. Cosmochim. Acta* **53**, 3045–3057.

Alexander C. M. O'D. (1993) Presolar SiC in chondrites – How variable and how many sources? *Geochim. Cosmochim. Acta* **57**, 2869–2888.

Alexander C. M. O'D. (1994) Evidence for short SiC lifetimes in the ISM. *Lunar Planet. Sci. XXV*. Lunar Planet. Inst., Houston. #9–10 (abstr.).

Alexander C. M. O'D. (2005) Re-examining the role of chondrules in producing the elemental fractionations in chondrites. *Meteorit. Planet. Sci.* **40**, 943–965.

Alexander C. M. O'D., Arden J. W., Ash R. D. and Pillinger C. T. (1990a) Presolar components in the ordinary chondrites. *Earth Planet. Sci. Lett.* **99**, 220–229.

Alexander C. M. O'D., Swan P. and Walker R. M. (1990b) In situ measurement of interstellar silicon carbide in two CM chondrite meteorites. *Nature* **348**, 715–717.

Alexander C. M. O'D., Boss A. P. and Carlson R. W. (2001) The early evolution of the inner solar system: a meteoritic perspective. *Science* **293**, 64–68.

Alexander C. M. O'D., Fogel M., Yabuta H. and Cody G. D. (2007) The origin and evolution of chondrites recorded in the elemental and isotopic compositions of their macromolecular organic matter. *Geochim. Cosmochim. Acta* **71**, 4380–4403.

Alexander C. M. O'D., Howard K. T., Bowden R. and Fogel M. L. (2013) The classification of CM and CR chondrites using bulk H, C and N abundances and isotopic compositions. *Geochim. Cosmochim. Acta* **123**, 244–260.

Alexander C. M. O'D., Cody G. D., Kebukawa Y., Bowden R., Fogel M. L., Kilcoyne A. L. D., Nittler L. R. and Herd C. D. K. (in press) Elemental, isotopic and structural changes in Tagish Lake insoluble organic matter produced by parent body processes. *Meteorit. Planet. Sci.*

Amari S., Lewis R. S. and Anders E. (1994) Interstellar grains in meteorites: I. Isolation of SiC, graphite and diamond; size distributions of SiC and graphite. *Geochim. Cosmochim. Acta* **58**, 459–470.

Anders E. and Zinner E. (1993) Interstellar grains in primitive meteorites – diamond, silicon carbide, and graphite. *Meteoritics* **28**, 490–514.

Baker L., Franchi I. A., Wright I. P. and Pillinger C. T. (2002) The oxygen isotopic composition of water from Tagish Lake: its relationship to low-temperature phases and to other carbonaceous chondrites. *Meteorit. Planet. Sci.* **37**, 977–985.

Bonal L., Quirico E., Bourot-Denise M. and Montagnac G. (2006) Determination of the petrologic type of CV3 chondrites by Raman spectroscopy of included organic matter. *Geochim. Cosmochim. Acta* **70**, 1849–1863.

Bose M., Floss C., Stadermann F. J., Stroud R. M. and Speck A. K. (2012) Circumstellar and interstellar material in the CO3

chondrite ALHA 77307: an isotopic and elemental investigation. *Geochim. Cosmochim. Acta* **93**, 77–101.

Brearley A. J. (1993) Matrix and fine-grained rims in the unequilibrated CO3 chondrite, ALHA 77307: origins and evidence for diverse, primitive nebular dust components. *Geochim. Cosmochim. Acta* **57**, 1521–1550.

Brearley A. J. (2006) The action of water. In *Meteorites and the Early Solar System II* (eds. D. S. Lauretta and H. Y. McSween). Univ. Arizona Press, Tucson, pp. 587–622.

Busemann H., Young A. F., Alexander C. M. O'D., Hoppe P., Mukhopadhyay S. and Nittler L. R. (2006) Interstellar chemistry recorded in organic matter from primitive meteorites. *Science* **312**, 727–730.

Busemann H., Alexander C. M. O'D. and Nittler L. R. (2007) Characterization of insoluble organic matter in primitive meteorites by microRaman spectroscopy. *Meteorit. Planet. Sci.* **42**, 1387–1416.

Busemann H., Nguyen A. N., Cody G. D., Hoppe P., Kilcoyne A. L. D., Stroud R. M., Zega T. J. and Nittler L. R. (2009) Ultraprimitive interplanetary dust particles from the comet 26P/Grigg-Skjellerup dust stream collection. *Earth Planet. Sci. Lett.* **288**, 44–57.

Cameron A. G. W. (1962) The formation of the sun and planets. *Icarus* **1**, 13–69.

Clayton R. N. and Mayeda T. K. (1984) The oxygen isotope record in Murchison and other carbonaceous chondrites. *Earth Planet. Sci. Lett.* **67**, 151–161.

Cody G. D. and Alexander C. M. O'D. (2005) NMR studies of chemical structural variation of insoluble organic matter from different carbonaceous chondrite groups. *Geochim. Cosmochim. Acta* **69**, 1085–1097.

Cody G. D., Alexander C. M. O'D. and Tera F. (2002) Solid state (^{1}H and ^{13}C) NMR spectroscopy of the insoluble organic residue in the Murchison meteorite: a self-consistent quantitative analysis. *Geochim. Cosmochim. Acta* **66**, 1851–1865.

Cody G. D., Alexander C. M. O'D., Yabuta H., Araki T. and Kilcoyne A. L. D. (2006) Complexity in the early Solar System as recorded in meteoritic organic matter. *Lunar Planet. Sci. XXXVII*. Lunar Planet. Inst., Houston. #1795 (abstr.).

Cody G. D., Alexander C. M. O'D., Yabuta H., Kilcoyne A. L. D., Araki T., Ade H., Dera P., Fogel M., Militzer B. and Mysen B. O. (2008) Organic thermometry for chondritic parent bodies. *Earth Planet. Sci. Lett.* **272**, 446–455.

Davidson J. (2009) NanoSIMS and beyond – Presolar grains in primitive meteorites and early Solar System formation. Ph. D. thesis, Open University. pp. 328.

Davidson J., Busemann H., Alexander C. M. O'D., Nittler L. R., Hoppe P., Franchi I. A. and Grady M. M. (2008) Were presolar grains destroyed by the nebular process responsible for the volatile element fractionation? *Lunar Planet. Sci. XXXIX*. Lunar Planet. Inst., Houston. #1184 (abstr.).

Davidson J., Busemann H., Alexander C. M. O'D., Nittler L. R., Schrader D. L., Orthous-Daunay F. R., Quirico E., Franchi I. A. and Grady M. M. (2009a) Presolar SiC abundances in primitive meteorites by NanoSIMS raster ion imaging of insoluble organic matter. *Lunar Planet. Sci. XL*. Lunar Planet. Inst., Houston. #1853 (abstr.).

Davidson J., Schrader D. L., Busemann H., Franchi I. A., Greenwood R. C., Alexander C. M. O'D., Lauretta D. S., Verchovsky A., Connolly H. C. and Grady M. M. (2009b) RBT 04133: a new, unusual carbonaceous chondrite. *Meteorit. Planet. Sci.* Suppl. #5141 (abstr.).

Davidson J., Busemann H. and Franchi I. A. (2012a) Presolar grain inventory of a fine-grained chondrule rim in CO3.0 chondrite ALHA 77307. *Meteorit. Planet. Sci. Suppl.* #5269 (abstr.).

Davidson J., Busemann H. and Franchi I. A. (2012b) A NanoSIMS and Raman spectroscopic comparison of interplanetary dust particles from comet Grigg-Skjellerup and non-Grigg Skjellerup collections. *Meteorit. Planet. Sci.* **47**, 1748–1771.

Floss C. and Stadermann F. J. (2005) Presolar (circumstellar and interstellar) phases in Renazzo: the effects of parent body processing. *Lunar Planet. Sci. XXXVI*. Lunar Planet. Inst., Houston. #1390 (abstr.).

Floss C. and Stadermann F. J. (2009a) High abundances of circumstellar and interstellar C-anomalous phases in the primitive CR3 chondrites QUE 99177 and MET 00426. *Astrophys. J.* **697**, 1242–1255.

Floss C. and Stadermann F. J. (2009b) Auger Nanoprobe analysis of presolar ferromagnesian silicate grains from primitive CR chondrites QUE 99177 and MET 00426. *Geochim. Cosmochim. Acta* **73**, 2415–2440.

Gao X., Amari S., Messenger L. R., Nittler L. R., Swan P. D. and Walker R. M. (1996) Survey of circumstellar grains in the unique carbonaceous chondrite Acfer 094. *Meteorit. Planet. Sci.* **31**, A48.

Gehrels N. (1986) Confidence limits for small numbers of events in astrophysical data. *Astrophys. J.* **303**, 336–346.

Gilmour I. (2003) Structural and isotopic analysis of organic matter in carbonaceous chondrites. In *Meteorites, Comets, and Planets* (ed. A. M. Davis) Vol. 1. *Treatise on Geochemistry* (eds. H. D. Holland and K. K. Turekian). Elsevier-Pergamon, Oxford. pp. 269–280.

Guo W. (2009) Carbonate clumped isotope thermometry: application to carbonaceous chondrites and effects of kinetic isotope fractionation. Ph. D. thesis, California Institute of Technology. pp. 243.

Guo W. and Eiler J. M. (2007) Temperatures of aqueous alteration and evidence for methane generation on the parent bodies of the CM chondrites. *Geochim. Cosmochim. Acta* **71**, 5565–5575.

Haenecour P. and Floss C. (2012) Stardust in fine-grained chondrule rims and matrix in LaPaz 031117: insights into the conditions of dust accretion in the solar nebula. *Lunar Planet. Sci. XLIII*. Lunar Planet. Inst., Houston. #1107 (abstr.).

Hoppe P., Amari S., Zinner E., Ireland T. and Lewis R. S. (1994) Carbon, nitrogen, magnesium, silicon and titanium isotopic compositions of single interstellar silicon carbide grains from the Murchison carbonaceous chondrite. *Astrophys. J.* **430**, 870–890.

Hoppe P., Cohen S. and Meibom A. (2013) NanoSIMS: technical aspects and applications in cosmochemistry and biological geochemistry. *Geostand. Geoanal. Res.* **37**, 111–154.

Howard K. T. and Alexander C. M. O'D. (2013) A new classification scheme for aqueously altered carbonaceous chondrites based on total phyllosilicates abundance. *Lunar Planet. Sci. XLIV*. Lunar Planet. Inst., Houston. #2598 (abstr.).

Huss G. R. (1990) Ubiquitous interstellar diamond and SiC in primitive chondrites – abundances reflect metamorphism. *Nature* **347**, 159–162.

Huss G. R. and Lewis R. S. (1994) Noble gases in presolar diamonds. I: Three distinct components. *Meteoritics* **29**, 791–810.

Huss G. R. and Lewis R. S. (1995) Presolar diamond, SiC, and graphite in primitive chondrites: abundances as a function of meteorite class and petrologic type. *Geochim. Cosmochim. Acta* **59**, 115–160.

Huss G. R., Lewis R. S. and Hemkin S. (1996) The "normal planetary" noble gas component in primitive chondrites: compositions, carrier and metamorphic history. *Geochim. Cosmochim. Acta* **60**, 3311–3340.

Huss G. R., Meshik A. P., Smith J. B. and Hohenberg C. M. (2003) Presolar diamond, silicon carbide, and graphite in carbonaceous

chondrites: implications for thermal processing in the solar nebula. *Geochim. Cosmochim. Acta* **67**, 4823–4848.

Huss G. R., Rubin A. E. and Grossman J. N. (2006) Thermal metamorphism in chondrites. In *Meteorites and the Early Solar System II* (eds. D. S. Lauretta and H. Y. McSween). Univ. Arizona Press, Tucson, pp. 567–586.

Hutchison R., Alexander C. M. O'D. and Barber D. J. (1987) The Semarkona meteorite: first recorded occurrence of smectite in an ordinary chondrite, and its implications. *Geochim. Cosmochim. Acta* **51**, 1875–1882.

Hynes K. M. and Gyngard F. (2009) The presolar grain database: http://presolar.wustl.edu/~pgd. *Lunar Planet. Sci. XL*. Lunar Planet. Inst., Houston. #1198 (abstr.).

Ishii H. A., Bradley J. P., Dai Z. R., Chi M., Kearsley A. T., Burchell M. J., Browning N. D. and Molster F. (2008) Comparison of comet 81P/Wild 2 dust with interplanetary dust from comets. *Science* **319**, 447–450.

Kerridge J. F. (1983) Isotopic composition of carbonaceous-chondrite kerogen: evidence for an interstellar origin of organic matter in meteorites. *Earth Planet. Sci. Lett.* **64**, 186–200.

Kuebler K. E., McSween H. Y., Carlson W. D. and Hirsch D. (1999) Sizes and masses of chondrules and metal-troilite grains in ordinary chondrites: possible implications for nebular sorting. *Icarus* **141**, 96–106.

Lambert D. L., Gustafsson B., Eriksson K. and Hinkle K. H. (1986) The chemical composition of carbon stars. I. Carbon, nitrogen, and oxygen in 30 cool carbon stars in the galactic disk. *Astrophys. J. Suppl.* **62**, 373–425.

Leitner J., Hoppe P. and Zipfel J. (2012a) The stardust inventories of Graves Nunataks 95229 and Renazzo: Implications for the distribution of presolar grains in CR chondrites. *Lunar Planet. Sci. XLIII*. Lunar Planet. Inst., Houston. #1835 (abstr.).

Leitner J., Vollmer C., Hoppe P. and Zipfel J. (2012b) Abundant primitive phases in fine-grained chondrule rims of CR and related chondrites. *Meteorit. Planet. Sci. Suppl.* #5191 (abstr.).

Leitner J., Vollmer C., Hoppe P. and Zipfel J. (2012c) Characterization of presolar material in the CR chondrite Northwest Africa 852. *Astrophys. J.* **745**, 38–53.

Lewis R. S., Ming T., Wacker J. F., Anders E. and Steel E. (1987) Interstellar diamonds in meteorites. *Nature* **326**, 160–162.

Lewis R. S., Amari S. and Anders E. (1994) Interstellar grains in meteorites: II. SiC and its noble gases. *Geochim. Cosmochim. Acta* **58**, 471–494.

Nagashima K., Krot A. N. and Yurimoto H. (2004) Stardust silicates from primitive meteorites. *Nature* **428**, 921–924.

Newton J., Bischoff A., Arden J. W., Franchi I. A., Geiger T., Greshake A. and Pillinger C. T. (1995) Acfer 094, a uniquely primitive carbonaceous chondrite from the Sahara. *Meteoritics* **30**, 47–56.

Nguyen A. N., Stadermann F. J., Zinner E., Stroud R. M., Alexander C. M. O'D. and Nittler L. R. (2007) Characterization of presolar silicate and oxide grains in primitive carbonaceous chondrites. *Astrophys. J.* **656**, 1223–1240.

Nguyen A. N., Nittler L. R., Stadermann F. J., Stroud R. M. and Alexander C. M. O'D. (2010) Coordinated analyses of presolar grains in the Allan Hills 77307 and Queen Elizabeth Range 99177 meteorites. *Astrophys. J.* **719**, 166–189.

Nittler L. R. (2003) Presolar stardust in meteorites: recent advances and scientific frontiers. *Earth Planet. Sci. Lett.* **209**, 259–273.

Nittler L. R. and Alexander C. M. O'D. (2003) Automated isotopic measurements of micron-sized dust: application to meteoritic presolar silicon carbide. *Geochim. Cosmochim. Acta* **67**, 4961–4980.

Nittler L. R., Alexander C. M. O'D., Gallino R., Hoppe P., Nguyen A. N., Stadermann F. J. and Zinner E. K. (2008) Aluminum-, calcium- and titanium-rich oxide stardust in ordinary chondrite meteorites. *Astrophys. J.* **682**, 1450–1478.

Orthous-Daunay F.-R. (2011) Empreinte moléculaire des processus post-accrétionnels dans la matière organique des chondrites carbonées. Ph. D. thesis, Université de Grenoble. pp. 162.

Orthous-Daunay F.-R., Quirico E., Brissaud O. and Schmitt B. (2008) Micro-infrared spectroscopy of insoluble organic matter extracted from primitive chondrites. *Meteorit. Planet. Sci.* **43**, A123.

Orthous-Daunay F.-R., Quirico E., Lemelle L., Beck P., deAndrade V., Simionovici A. and Derenne S. (2010) Speciation of sulfur in the insoluble organic matter from carbonaceous chondrites by XANES spectroscopy. *Earth Planet. Sci. Lett.* **300**, 321–328.

Pizzarello S., Cooper G. W. and Flynn G. J. (2006) The nature and distribution of the organic material in carbonaceous chondrites and interplanetary dust particles. In *Meteorites and the Early Solar System II* (eds. D. S. Lauretta and H. Y. McSween). Univ. Arizona Press, Tucson, pp. 625–651.

Qin L., Nittler L. R., Alexander C. M. O'D., Wang J., Stadermann F. J. and Carlson R. W. (2011) Extreme ^{54}Cr-rich nano-oxides in the CI chondrite Orgueil – implication for a late supernova injection into the Solar System. *Geochim. Cosmochim. Acta* **75**, 629–644.

Quirico E., Raynal P. I. and Bourot-Denise M. (2003) Metamorphic grade of organic matter in six unequilibrated ordinary chondrites. *Meteorit. Planet. Sci.* **38**, 795–811.

Quirico E., Borg J., Raynal P. I., Montagnac G. and d'Hendecourt L. (2005) A micro-Raman survey of 10 IDPs and 6 carbonaceous chondrites. *Planet. Space Sci.* **53**, 1443–1448.

Reynolds J. H. and Turner G. (1964) Rare gases in the chondrite Renazzo. *J. Geophys. Res.* **69**, 3263–3281.

Russell S. S., Ott U., Alexander C. M. O'D., Zinner E. K., Arden J. W. and Pillinger C. T. (1997) Presolar silicon carbide from the Indarch (EH4) meteorite: comparison with silicon carbide populations from other meteorite classes. *Meteorit. Planet. Sci.* **32**, 719–732.

Robert F. and Epstein S. (1982) The concentration and isotopic composition of hydrogen, carbon and nitrogen in carbonaceous meteorites. *Geochim. Cosmochim. Acta* **46**, 81–95.

Schrader D. L., Franchi I. A., Connolly, Jr., H. C., Greenwood R. C., Lauretta D. S. and Gibson J. M. (2011) The formation and alteration of the Renazzo-like carbonaceous chondrites I: implications of bulk-oxygen isotopic composition. *Geochim. Cosmochim. Acta* **75**, 308–325.

Scott E. R. D. and Haack H. (1993) Chemical fractionation in chondrites by aerodynamic sorting of chondritic materials. *Meteoritics* **28**, A434.

Sestak S., Franchi I. A., Verchovsky A. B., Al-Kuzee J., Braithwaite N. St J. and Burnett D. S. (2006). Application of semiconductor industry cleaning technologies for Genesis sample collectors. *Lunar Planet. Sci. XXXVII*. Lunar Planet. Inst., Houston. #1878 (abstr.).

Signer P. and Suess H. E. (1963) Rare gases in the sun, in the atmosphere, and in meteorites. In *Earth Science and Meteorites* (eds. J. Geiss and E. D. Goldberg). North Holland, Amsterdam, pp. 241–272.

Stadermann F. J., Floss C. and Wopenka B. (2006) Circumstellar aluminum oxide and silicon carbide in interplanetary dust particles. *Geochim. Cosmochim. Acta* **70**, 6168–6179.

Tang M. and Anders E. (1988) Isotopic anomalies of Ne, Xe, and C in meteorites. II. Interstellar diamond and SiC: carriers of exotic noble gases. *Geochim. Cosmochim. Acta* **52**, 1235–1244.

Verchovsky A. B., Wright I. P. and Pillinger C. T. (2004) Astrophysical significance of asymptotic giant branch stellar

wind energies recorded in meteoritic SiC grains. *Astrophys. J.* **607**, 611–619.

Vollmer C., Brenker F., Hoppe P. and Stroud R. M. (2009) Direct laboratory analysis of silicate stardust from red giant stars. *Astrophys. J.* **700**, 774–782.

Weisberg M. K. and Huber H. (2007) The GRO 95577 CR1 chondrite and hydration of the CR parent body. *Meteorit. Planet. Sci.* **42**, 1495–1503.

Weisberg M. K., Prinz M., Clayton R. N. and Mayeda T. K. (1993) The CR (Renazzo-type) carbonaceous chondrite group and its implications. *Geochim. Cosmochim. Acta* **57**, 1567–1586.

Yang J. and Epstein S. (1983) Interstellar organic matter in meteorites. *Geochim. Cosmochim. Acta* **47**, 2199–2216.

Yang J. and Epstein S. (1984) Relic interstellar grains in Murchison meteorite. *Nature* **311**, 544–547.

Zanda B., Bland P. A., Le Guillou C. and Hewins R. H. (2009) Volatile element distribution in matrix and chondrules of carbonaceous and ordinary chondrites. *Lunar Planet. Sci.* **40**, #1810 (abstr.).

Zanda B., Humayun M. and Hewins R. H. (2012) Chemical composition of matrix and chondrules in carbonaceous chondrites: implications for disk transport. *Lunar Planet. Sci.* **43**, #2413.

Zhao X., Floss C., Lin Y. and Bose M. (2013) Stardust investigation into the CR chondrite Grove Mountain 021710. *Astrophys. J.* **769**, 49–64.

Zinner E. (2014) Presolar Grains. In *Meteorites, Comets, and Planets* (ed. A. M. Davis) (second ed.) Vol. 1. *Treatise on Geochemistry* (eds. H. D. Holland and K. K. Turekian). Elsevier. Oxford. pp. 181–213.

Zinner E., Ming T. and Anders E. (1989) Interstellar SiC in the Murchison and Murray meteorites: Isotopic composition of Ne, Xe, Si, C, and N. *Geochim. Cosmochim. Acta* **53**, 3273–3290.

Zolensky M. E., Mittlefehldt D. W., Lipschutz M. E., Wang M.-S., Clayton R. N., Mayeda T. K., Grady M. M., Pillinger C. and Barber D. (1997) CM chondrites exhibit the complete petrologic range from type 2 to 1. *Geochim. Cosmochim. Acta* **61**, 5099–5115.

Zolensky M., Nakamura-Messenger K., Rietmeijer F., Leroux H., Mikouchi T., Ohsumi K., Simon S., Grossman L., Stephan T., Weisberg M., Velbel M., Zega T., Stroud R., Tomeoka K., Ohnishi I., Tomioka N., Nakamura T., Matrajt G., Joswiak D., Brownlee D., Langenhorst F., Krot A., Kearsley A., Ishii H., Graham G., Dai Z. R., Chi M., Bradley J., Hagiya K., Gounelle M. and Bridges J. (2008) Comparing Wild 2 particles to chondrites and IDPs. *Meteorit. Planet. Sci.* **43**, 261–272.

Associate editor: Anders Meibom